NAVAL POSTGRADUATE SCHOOL

Monterey, California

THESIS

STORE SEPARATION
METHODOLOGY ANALYSIS

by
Darcy Michael Hansen

September, 1991

Thesis Advisor: Prof. Oscar Biblarz
Co-Advisor: Prof. Louis Schmidt

Approved for public release; distribution is unlimited

REPORT DOCUMENTATION PAGE

1a REPORT SECURITY CLASSIFICATION Unclassified	1b RESTRICTIVE MARKINGS
2a SECURITY CLASSIFICATION AUTHORITY	3 DISTRIBUTION/AVAILABILITY OF REPORT Approved for public release; distribution is unlimited.
2b DECLASSIFICATION/DOWNGRADING SCHEDULE	
4 PERFORMING ORGANIZATION REPORT NUMBER(S)	5 MONITORING ORGANIZATION REPORT NUMBER(S)
6a NAME OF PERFORMING ORGANIZATION Naval Postgraduate School 6b OFFICE SYMBOL (*If applicable*) 31	7a NAME OF MONITORING ORGANIZATION Naval Postgraduate School
6c ADDRESS (*City, State, and ZIP Code*) Monterey, CA 93943-5000	7b ADDRESS (*City, State, and ZIP Code*) Monterey, CA 93943-5000
8a NAME OF FUNDING/SPONSORING ORGANIZATION 8b OFFICE SYMBOL (*If applicable*)	9 PROCUREMENT INSTRUMENT IDENTIFICATION NUMBER
8c ADDRESS (*City, State, and ZIP Code*)	10 SOURCE OF FUNDING NUMBERS Program Element No / Project No / Task No / Work Unit Accession Number

11 TITLE (*Include Security Classification*)
Store Separation Methodology Analysis

12 PERSONAL AUTHOR(S) Hansen, Darcy M.

13a TYPE OF REPORT	13b TIME COVERED	14 DATE OF REPORT (*year, month, day*)	15 PAGE COUNT
Master's Thesis	From To	1991, September	81

16 SUPPLEMENTARY NOTATION
The views expressed in this thesis are those of the author and do not reflect the official policy or position of the Department of Defense or the U.S. Government.

17 COSATI CODES			18 SUBJECT TERMS (*continue on reverse if necessary and identify by block number*)
FIELD	GROUP	SUBGROUP	separation, store, trajectory

19 ABSTRACT (*continue on reverse if necessary and identify by block number*)

Various computational methods and operational computer codes used to predict the aerodynamic coefficients and separation trajectories of aircraft stores are examined. The semi-empirical aeroprediction code Missile DATCOM is used to obtain the coefficients of a modeled store. These coefficients, together with the modeled ejection forces, are used in free-stream state-space equations of motion to predict the store trajectory. The results are compared with the Nielson Engineering and Research (NEAR) store separation code which provides accurate trajectory profiles, for speeds below the subsonic Mach critical speed, by use of a vortex-lattice and panel method. Modification of the Missile DATCOM aerodynamic coefficients provides single-point state-space prediction of the store pitch trajectory to within 30% of the NEAR code values. Store trajectories were restricted to the first 0.2 seconds of free-flight.

20 DISTRIBUTION/AVAILABILITY OF ABSTRACT	21 ABSTRACT SECURITY CLASSIFICATION	
[X] UNCLASSIFIED/UNLIMITED [ ] SAME AS REPORT [ ] DTIC USERS	Unclassified	
22a NAME OF RESPONSIBLE INDIVIDUAL Prof. Oscar Biblarz	22b TELEPHONE (*Include Area code*) (408) 646-3096	22c OFFICE SYMBOL AA/BI

DD FORM 1473, 84 MAR — 83 APR edition may be used until exhausted; All other editions are obsolete

Approved for public release; distribution is unlimited.

Store Separation
Methodology Analysis

by

Darcy M. Hansen
B.S., Arizona State University, 1983

Submitted in partial fulfillment
of the requirements for the degree of

MASTER OF SCIENCE IN AERONAUTICAL ENGINEERING

from the

NAVAL POSTGRADUATE SCHOOL
September 1991

ABSTRACT

Various computational methods and operational computer codes used to predict the aerodynamic coefficients and separation trajectories of aircraft stores are examined. The semi-empirical aeroprediction code Missile DATCOM is used to obtain the coefficients of a modeled store. These coefficients, together with the modeled ejection forces, are used in free-stream state-space equations of motion to predict the store trajectory. The results are compared with the Nielson Engineering and Research (NEAR) store separation code which provides accurate trajectory profiles, for speeds below the critical speed, by use of a vortex-lattice and panel method. Modification of the Missile DATCOM aerodynamic coefficients provides single-point state-space prediction of the store pitch trajectory within 30% of the NEAR code results. Store trajectories were restricted to the first 0.2 seconds of free flight.

TABLE OF CONTENTS

I. STORE SEPARATION INTRODUCTION 1

A. BACKGROUND 1

B. MATHEMATICAL MODELING 2

C. METHODOLOGY 3

II. EJECTION FORCES AND MOMENTS 5

A. EJECTOR CHARACTERISTICS 5

B. FORCES 8

1. Theory 8

2. Example 8

C. MOMENTS 9

1. Theory 9

2. Example 9

D. PRELIMINARY OBSERVATION 10

III. AERODYNAMIC CALCULATION 11

A. THEORY 11

1. Longitudinal Equations 12

2. Lateral Equations 13

3. State Variable Representation 14

B. MISDATCOM 15

1. Theory 15

2. Procedure 17
C. AERODYNAMIC CALCULATION 20
1. Longitudinal 20
2. Lateral 23
D. PARAMETER VARIATION 23
E. PRELIMINARY OBSERVATION 24

IV. "NEAR" PROGRAM 25
A. BACKGROUND 25
B. THEORY 26
1. Source Program 26
2. Trajectory Program 27
3. Shape Modeling 28
C. PROCEDURE 31
1. Source Program 31
2. Trajectory Program 35

V. RESULTS AND COMPARISONS 40
A. EJECTOR FORCES AND MOMENTS 40
1. Vertical Velocity 40
2. Pitch Rate Q 40
B. TRAJECTORY COMPARISON 40
1. Vertical Separation Z 41
2. Pitch Angle 41
3. Pitch Rate 45
4. Vertical Velocity 45

C. AUGMENTED AEROPREDICTION 45

1. C_{Mq}- Coefficient 46

2. $C_{M\dot{\alpha}}$- Coefficient 46

3. Trajectory Prediction 46

VI. CONCLUSIONS 50

APPENDIX A 52

APPENDIX B 53

APPENDIX C 55

APPENDIX D 60

APPENDIX E 61

LIST OF REFERENCES 66

INITIAL DISTRIBUTION LIST 68

LIST OF FIGURES

Figure 1 Ejector Force 7

Figure 2 MISDATCOM Pod Shape 18

Figure 3 MISDATCOM Input 18

Figure 4 MISDATCOM Output 19

Figure 5 Pitch Angle Response 21

Figure 6 Pitch Rate Response 21

Figure 7 Vertical Separation Distance 22

Figure 8 Vertical Velocity 22

Figure 9 F/A18 NEAR Polynomials 29

Figure 10 Source Program Input 32

Figure 11 Source Program Output 34

Figure 12 Trajectory Program Partial Output 37

Figure 13 Trajectory Output (Cont) 38

Figure 14 Vertical Separation Distance 43

Figure 15 Pitch Angle 43

Figure 16 Parameter Error 44

Figure 17 Vertical Separation Distance (Augmented) . 48

Figure 18 Pitch Angle (Augmented) 48

Figure 19 Pitch Rate (Augmented) 49

Figure 20 Parameter Error (Augmented) 49

Figure 21 Store Reference Frame 55

Figure 22 Control-C Program For EOM Simulation . . . 60

Figure 23 MISDATCOM INPUT/OUTPUT 61

Figure 24 MISDATCOM Input/Output (Cont) 62
Figure 25 MISDATCOM Input/Output (Cont) 63
Figure 26 MISDATCOM Input/Output (Cont) 64
Figure 27 MISDATCOM Input/Output (Cont) 65

LIST OF ABBREVIATIONS AND ACRONYMS

C_A	axial force coefficient
C_D	drag coefficient
C_L	lift coefficient
C_{LN}	yawing-moment coefficient
C_{lL}	rolling-moment coefficient
C_{NA}	normal-force derivative wrt to AOA
C_{MA}	pitching-moment derivative wrt to AOA
$C_{Y\beta}$	side-force derivative wrt to beta
$C_{lN\beta}$	yawing-moment derivative wrt to beta
$C_{lL\beta}$	rolling-moment derivative wrt to beta
C_m	pitching-moment coefficient
$C_{m\dot{\alpha}}$	pitching-moment derivative wrt to AOA rate
C_{mq}	pitching-moment derivative wrt to pitch rate
C_n	yawing-moment coefficient
C_N	normal-force coefficient
$C_{N\dot{\alpha}}$	normal-force derivative wrt to AOA rate
C_{Nq}	normal-force derivative wrt to pitch rate
C_Y	side-force coefficient
d	maximum store diameter
g	gravitational constant
I_{xx}	mass moment of inertia about the x-axis
I_{yy}	mass moment of inertia about the y-axis
I_{zz}	mass moment of inertia about the z-axis

l	body (or store) length
l_R	reference length
m	body contour slope
M_∞	free-stream Mach number
q_∞	free-stream dynamic pressure
S	local body cross-sectional area
S_R	reference area
t	time (seconds)
V_∞	free-stream velocity
x_s, y_s, z_s	store coordinate system
x_b, y_b, z_b	aircraft body coordinate system
α	fuselage or store angle of attack
β	fuselage or store sideslip angle

ACKNOWLEDGEMENT

I would like to thank the faculty of the Aeronautical and Astronautical Department at the Naval Postgraduate School for providing me with such professional insight into the field of aeronautics. I especially want to thank my thesis advisors, Prof. O. Biblarz and Prof. L. Schmidt, for continually providing guidance and direction in my search for the elusive truth.

Rony Salama, a fellow student, was also instrumental in validating my results by use of his practical knowledge in the field of store separation.

In addition, my thesis work would have been impossible without the able assistance of Tony Cricelli, who helped me navigate the labyrinth of computer paths.

And most importantly, I want to thank my wife, Victoria, for supporting her "ghost" husband for the duration of this thesis.

I. STORE SEPARATION INTRODUCTION

A. BACKGROUND

The prediction of the trajectory of a store ejected from an aircraft is of major concern to defense aviation. The increasing requirement for aircraft to fulfill a multiple role in the hostile environment demands that it also carry an ever-increasing variety of stores. These stores range from missiles and bombs stockpiled for many years to new, aerodynamically complex stores with lifting bodies.

The aim of this work is to review current methods of predicting store releases, compare results of two different methods, and to present an easy-to-use methodology for investigating the subsonic release of a unsophisticated store.

A non-axisymmetric pod ejected from the F/A-18 outboard pylon is presented as an example. This store was chosen because it is of practical value due to the extensive use of these modified pods at the Pacific Missile Test Center, at Point Mugu, California. Non-axisymmetrical stores are very difficult to model and present a special problem in the store separation field. This pod is, therefore, modeled as axisymmetric and non-axisymmetric, and the results are compared. In addition, the store lacks aerodynamic control surfaces and is highly unstable. Application of the

methodology presented here should eventually provide the user with accurate results for a minimal time and cost expenditure.

B. MATHEMATICAL MODELING

There are many ways to mathematically model store separation. Economics and accuracy are always the main considerations when exploring the codes and methods to be used. For simple cases, intermediate approaches such as panel methods and solutions of the Euler equations provide sufficient accuracy. Calculations involving flow separation and shock wave interference become too complex for intermediate methods and acceptable results can only be obtained using modern computational fluid dynamic (CFD) techniques involving solutions of the Navier-Stokes equations [Ref. 1:p. 7-2]. For speeds below the subsonic Mach critical speed, component buildup methods (empirical and semi-empirical), and panel methods provide the necessary accuracy and are much easier to use. The codes chosen for this study are explained in detail in their respective sections.

The F/A-18 model was obtained from Mr. L. L. Gleason of the Ordnance Systems Department, Naval Weapons Center, at China Lake, California. The F/A-18 was chosen due to its wide variety of store carriage and also because of its solid future with Naval aviation.

The store model is based upon both the Missile Datcom method [Ref 2] and also by the Nielson program [Ref 3]. These

will be discussed in Sections III and IV. Appendix A contains the physical description of the pod and its inertial characteristics.

C. METHODOLOGY

The initial investigation (Section II) consisted of looking at the ejector forces, combined with the store's inertial characteristics, to give a sense of the magnitude of initial velocities and moments. These forces and moments, while easy to predict, were insufficient to provide real evidence of a safe release or of a release problem. A large pitch-down moment or a large vertical velocity may be off-set by unforeseen aerodynamic forces. The velocities and moments calculated will be used in Section III and compared with results of Section IV for trajectory prediction.

Section III introduces a method of predicting the store's longitudinal and lateral aerodynamic coefficients using a missile code (Missile DATCOM) developed by McDonnell Douglas Missile Systems Company for the Flight Dynamics Laboratory (FDL), Wright-Patterson Air Force Base (WFAFB), Ohio [Ref. 2]. These aerodynamic coefficients are then used in longitudinal and lateral equations of motion to predict the free-stream trajectory of the store. A brief explanation of the derivation of these equations of motion is provided to the reader. An accurate representation of the aerodynamic characteristics is essential for the full prediction of the

shape's trajectory. Missile DATCOM is based on the body buildup method and includes a number of prediction methods for each component of the configuration. Other codes, such as MISL3, are also available, each with its own relative strengths.

Section IV describes a computer prediction method developed by Nielson Engineering and Research, Inc., (NEAR), also under contract to the United States Air Force. This code provides a six degree-of-freedom (6DOF) simulation which takes into account the aircraft flowfield using vortex-lattice and panel methods. The NEAR simulation provides a high fidelity representation for the subsonic case, but also requires the most effort and computer capability. An attempt has been made to minimize the complexity of the input to the program. Once a good data base has been developed the NEAR code should prove easy to use. It has been used extensively throughout the defense industry, and has undergone many modifications to incorporate improvements and options.

Section V compares the trajectory results of the linearized aerodynamic simulation method and the NEAR code. A modification to the linear coefficients used in the linear aerodynamic simulation is also discussed.

II. EJECTION FORCES AND MOMENTS

Although quite uncomplicated in nature, calculating the ejection forces and moments provides the user with a feel for the magnitude of the initial movement of the store. This procedure should be done prior to using any other method as a preliminary step in order to prepare for the simulation.

A. EJECTOR CHARACTERISTICS

The non-aerodynamic forces involved in the ejection of a store depend upon the ejector cartridge, the ejector rack, the weight of the store, and the rigidity of the wing. Each of these parameters determine the resultant moments and forces provided to the store. The store and the wing (or fuselage) were considered as rigid, thus neglecting any aeroelastic or structural bending effects. None of the methods discussed here address aeroelastic bending due to the added complexity of the problem.

The Douglas production BRU-32/A Bomb Ejector Rack combines two sets of hooks, one set at 14-inch spacing and one set at 30-inch spacing, with an ejection system designed for carriage of stores with suspension lugs per MIL-A-8591. Two electrically initiated CCU-45B cartridges are used for store release and ejection. The self-retracting ejector pistons,

spaced symmetrically 20 inches apart at each end of the rack, have a piston stroke of six inches. These pistons are spring loaded against the store during loading to prevent impact of pistons during firing. The orifice sizes can be varied, by replacement, to provide force and pitch control for store separation. [Ref. 4]

The best source of ejector data is from the Aircraft Ordnance Procedures (AOP) contained in the Aircraft Stores Interface Manual, (Reference 4). This manual contains a complete description of the rack under consideration. Here, the example separation uses two 14-inch spaced hooks and 0.118-Diameter orifices. The force diagram corresponding to this orifice, modeled from the AOP, is shown in Figure 1. Sufficient data points were read from the AOP graph in order to curve-fit the points using Computer Associates' CricketGraph® software [Ref. 5]. This provided two things; 1.) integration of the polynomial equation gave the total impulse value, and 2.) Nielson software in Section IV uses a fifth-order polynomial for calculations. Note that the AOP shows the total force provided by the ejector, while the NEAR simulation requires a force-per-ejector-foot polynomial. Given the shape of the force curve, a triangular representation of the curve gave a value of 348 lb_f-sec versus the integrated value of 344.9 lb_f-sec, which corresponds to an error of only 1%. Therefore elementary estimates of the total impulse are practical.

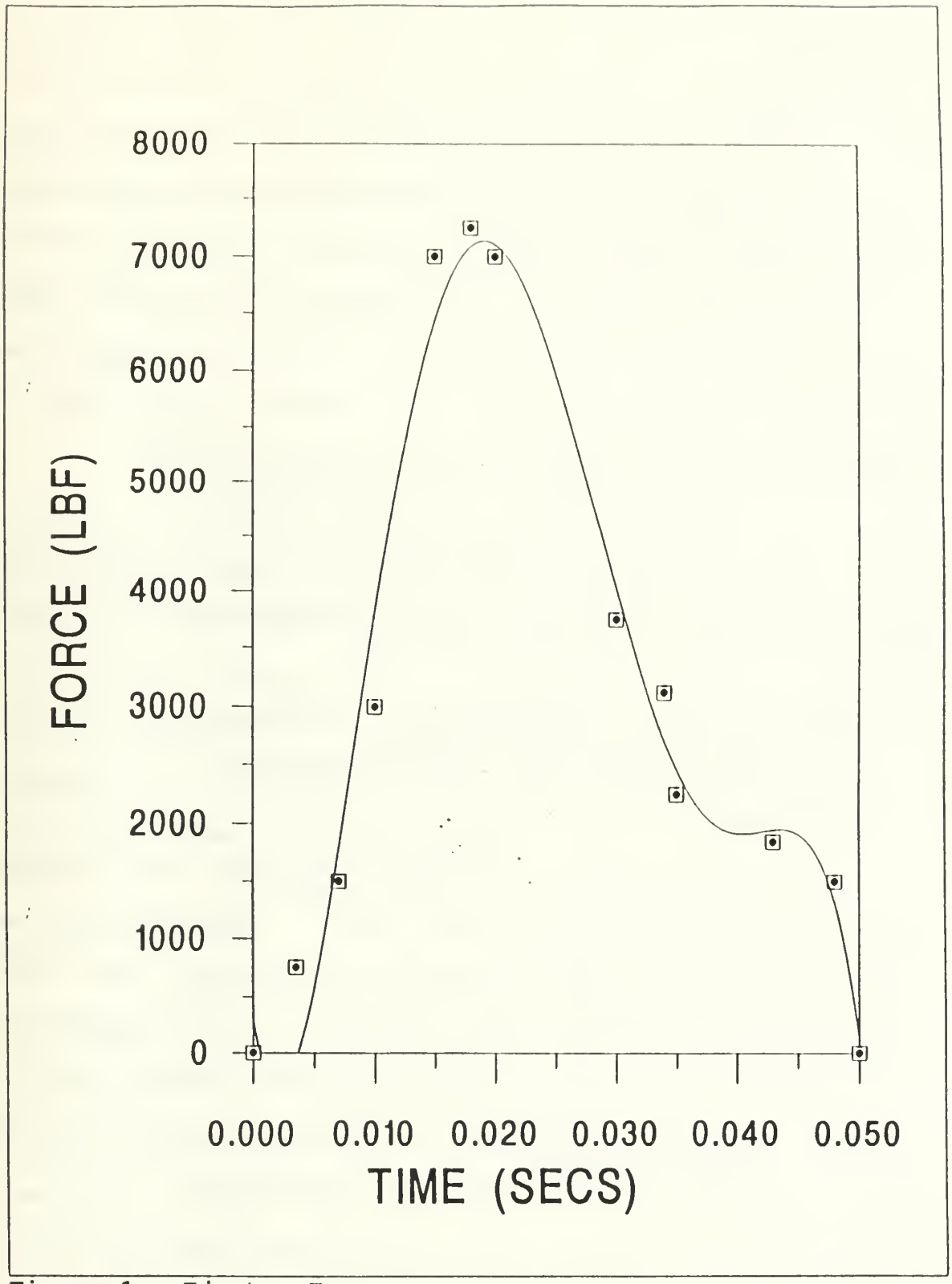

Figure 1 Ejector Force

B. FORCES

1. Theory

Using the conservation of linear momentum theory presented in Appendix B, the pod was modeled as a simple beam. The weight was concentrated at the center of gravity and the resultant ejection forces were placed at the ejector feet locations. The ejection force time histories are treated as an equivalent force impulse which results in a change in linear momentum as shown by the following equation:

$$\int \Sigma F_z \, dt = G_2 - G_1 = (M*V_z)_2 - (M*V_z)_1$$

The integral for representing the linear impulse is based upon the fifth-order polynomial force time history shown here.

$$y = 280.2 - 608022.8x + 180688545.8x^2 - 10638451765.5x^3 + 234526098234.3x^4 - 1783873760363.4x^5$$

2. Example

For our example, the BRU-32A bomb rack used two CCU-45B cartridge-activated devices (CADS). The peak force was 14,500 lb_f and the pulse duration was 50 msec. The total linear impulse calculated was 345 lb_f-sec. Using a weight of 371 pounds for the pod, the end-of-stroke velocity was 29.9 feet per sec (fps). This value was used in Section III as the initial velocity for the trajectory simulation.

The graphs contained in the AOP shows end-of-stroke velocity for a 371 lb store to be approximately 24.5 fps. This graph is derived from empirical data and should provide the most accurate representation of the actual release velocity. The values of 24.5 and 29.9 fps are compared with the end-of-stroke store velocity of 30.9 fps predicted from the NEAR code in Section IV.

C. MOMENTS

1. Theory

The pod was modeled as a simple beam. The inertial characteristics of the store are listed in Appendix A. The two ejector feet provide the beam with a moment. The equations used are elementary, and with certain assumptions the angular velocity can be calculated. The equations are based on conservation of angular momentum. The equations and assumptions are presented in Appendix B for completeness. The resulting equation is shown here.

$$\int \Sigma M_y \, dt = I_{yy} * \dot{\omega}_y$$

2. Example

The center of gravity was offset aft of the center of the ejector feet by 4.05 inches. The impulse thus provided the pod with 1.12 radians per second (rps) or 64.1 deg/sec initial angular velocity. The question now is, are these reasonable values? At the end of 0.429 seconds, the shape will be one body-length below the aircraft. At the same time,

the shape will have rotated 27.5 degrees nosedown. Therefore, without considering the aerodynamics of the vehicle, the pod seems to have cleared the wing. A good rule of thumb is 2-3 body lengths clearance, although exceptions do occur.

D. PRELIMINARY OBSERVATION

This initial calculation provides an approximate estimate of the forces and moments involved. The values obtained are of sufficient accuracy for calculations such as end-of-stroke loading, etc. Excessively large separation velocities are usually an indication of a miscalculation. Translational velocities should range from 10-30 fps and pitching velocities from 0-6 rps.

III. AERODYNAMIC CALCULATION

A. THEORY

Many physical systems can be modeled by second-order differential equations. The mathematical treatment of fixed-wing flight vehicle motions was first developed by G.H. Bryan. He laid the mathematical foundation for airplane dynamic stability analysis, developed the concept of the aerodynamic stability derivative, and recognized that the equations of motion could be separated into a symmetric longitudinal motion and an unsymmetric lateral motion. Experimental studies were initiated by L. Bairstow and B.M. Jones of the National Physical Laboratory in England, and by Jerome Hunsaker of the Massachusetts Institute of Technology to determine estimates of the aerodynamic stability derivatives in Bryan's theory. In addition to determining stability derivatives from wind-tunnel tests of scale models, Bairstow and Jones nondimensionalized the equations of motion and showed that, with certain assumptions, there were two independent solutions, i.e., one longitudinal and one lateral. These two solutions provide the free-stream trajectories we seek. [Ref. 6:p. 113]

The dynamic stability characteristics of a pod can be represented by six equations of motion, three for the forces

involved X, Y, and Z and three for the moments L, M and N. The force equations relate the forces acting on the body to the corresponding linear accelerations and the moment equations relate the moments to the corresponding angular accelerations. It is usually possible to consider the longitudinal motions completely separately from the lateral-directional motion, by neglecting the various coupling terms. [Ref. 7:p. 14]

As a caveat to the use of this method, these equations are the linearized version and are only valid up to approximately 10 degrees angle-of-attack. Treatment of the non-linear aerodynamic coefficients, while not extremely difficult, does require knowledge of the behavior of the coefficients. Since the goal of this report is to predict the behavior of new shape configurations, this knowledge is not presumed. Therefore, the results obtained in this fashion are only valid for estimating the motion in the first fractions of a second. These results are compared with those obtained in the more rigorous method of Section IV.

1. Longitudinal Equations

The rigid-body, longitudinal equations of motion can be developed from Newton's second law:

$$\Sigma \text{Pitching moments} = \Sigma M_{cg} = I_{yy} * \ddot{\Theta}$$

The assumption that body motion consists of small deviations from its equilibrium flight condition allows us to use

perturbation theory to examine the aerodynamic force derivatives in terms of angle-of-attack (AOA), vertical velocity, pitch angle, and pitch rate, by means of a Taylor series expansion. The X-force, Z-force, and pitching moment equations comprise the longitudinal equations. To separate these equations from the lateral equations, they must not be coupled. This is a reasonable assumption given the nominal geometric shape of missiles or pods [Ref. 6]. The body is constrained to move in a vertical plane and is free to pitch about its center of gravity. For a comprehensive derivation of the equations of motion, see Reference 6. The resulting equations of motion are shown in Appendix C.

2. Lateral Equations

The Y-force, rolling, and yawing moment equations comprise the lateral equations of motion. Once again, these equations are uncoupled from the longitudinal equations by the assumption of small cross-component moments of inertia. That is, I_{xy}, I_{xz}, I_{yz} are small in comparison to the principal axis moments. These equations are also valid assuming only small variations in displacement and velocity. The lateral equations are derived from the following Newton's laws:

$$\Sigma \text{Rolling moments} = I_{xx} * \ddot{\Phi}$$

$$\Sigma \text{Yawing moments} = I_{zz} * \ddot{\psi}$$

The third equation is derived from the Taylor series expansion of the side force derivative. The lateral motion of the pod

disturbed from its equilibrium state is a complicated combination of rolling, yawing, and sideslipping motions. Assuming the cross products of inertia are ignored, some of the coupling terms can be simplified.

3. State Variable Representation

The linearized longitudinal and lateral equations developed above are simple, ordinary linear differential equations with constant coefficients. The coefficients in the differential equations are made up of the aerodynamic stability derivatives, mass, and inertia characteristics of the pod. These equations can be written as a set of first-order differential equations in the state-space (state variable) form:

$$\{\dot{x}\} = [A]*\{x\} + [B]*\{\eta\}$$

where $\{x\}$ is the state vector, $\{\eta\}$ is the control vector and the matrices [A] and [B] contain the pod's dimensional stability derivatives. In our case the pod does not have any active control surfaces. For missile launches, however, the control vector and the B-matrix would be used to represent the control surfaces and control input. The simplified state-space representations of the longitudinal and lateral equations of motion are shown in Appendix C. The required

coefficients listed in Appendix C are derived using the procedures in Section III.B.

The state-space representation of the equations of motion can be solved simultaneously using matrix software such as MATLAB® [Ref. 8] or Control-C® [Ref. 9]. Given the conditions of the ejection, namely, initial translational velocities, initial angular velocities, and attitude angles, solutions of the state-space equations can be used to predict the trajectory of the pod. The initial angles and velocities are the initial conditions imposed upon the state-space equations. The Control-C® commands for this procedure are contained in Appendix D.

B. MISDATCOM

MISDATCOM was developed by McDonnell Douglas Astronautics Company, St Louis, Missouri, for the Flight Dynamics Laboratory of the Air Force Wright Aeronautical Laboratories, Wright-Patterson AFB. The program was completed in December 1985. The Missile Datcom was created to provide an aerodynamic design tool which has the predictive accuracy suitable for preliminary design, and the capability for the user to easily substitute methods to fit specific applications. [Ref. 2:p. 1]

1. Theory

There are many different methods to predict the aerodynamic static, dynamic, and control characteristics of

missiles. Component build-up was chosen as the most suitable for this program. Although panel methods are better suited for arbitrary configurations, component build-up was chosen due to the accuracy provided for conventional configurations and for the ability to do parametric studies easier.

Basically, component build-up consists of using various methods to compute the characteristics (skin friction, force and moment coefficients, panel loading,...) of the individual configuration components. The various methods are chosen for their applicability to the configuration or flight condition. Then the components are combined. Previous methods of combining the components (fins, body, engine inlet) consisted of adding the individual coefficients and then multiplying the sum by some interference factor obtained using slender body theory. The approach taken with MISDATCOM was to use the "equivalent angle of attack method" developed by Nielson Engineering and Research, Inc. (NEAR). This method assumes that the panel loading for a given panel angle-of-attack is unique. With this method the panel angle of attack is computed including the effect of panel roll orientation with respect to the free stream velocity vector, panel proximity to the fuselage or to other panels, and external vortex flow field effects. Then the isolated panel characteristics are interpolated at the panel equivalent angle of attack to yield the panel load when mounted on a body in combination with other surfaces. [Ref. 2]

2. Procedure

The procedure for using MISDATCOM is straightforward. The pod shape is modeled using simple geometric shapes. The previous release of MISDATCOM software could only handle axisymmetric shapes or forms with a vertical plane of symmetry. Unfortunately, the pod under consideration is non-axisymmetric and therefore the results are not entirely valid. The latest version, however, can model some non-axisymmetry through the use of a "protuberance" option. This is the April 1991 release and is now available.

For this investigation, a simulation run was made using both versions and a comparison of the aerodynamic coefficients was made. The pod radius was also varied from the minimum pod to the maximum, and the resulting coefficients compared. The MISDATCOM code coefficients were somewhat insensitive to radius changes of this magnitude, therefore, the minimum-radius, axisymmetric case was retained for comparison with the minimum-radius non-axisymmetric case. Figure 2 shows the pod semi-profile of the MISDATCOM procedure alongside the pod semi-profile of the NEAR simulation. Figure 3 contains a sample input to the program and Figure 4 lists a partial sample output. The actual input and output of the program are contained in Appendix E. These aerodynamic coefficients are next used in the longitudinal and lateral state-space equations of motion to predict the store trajectory.

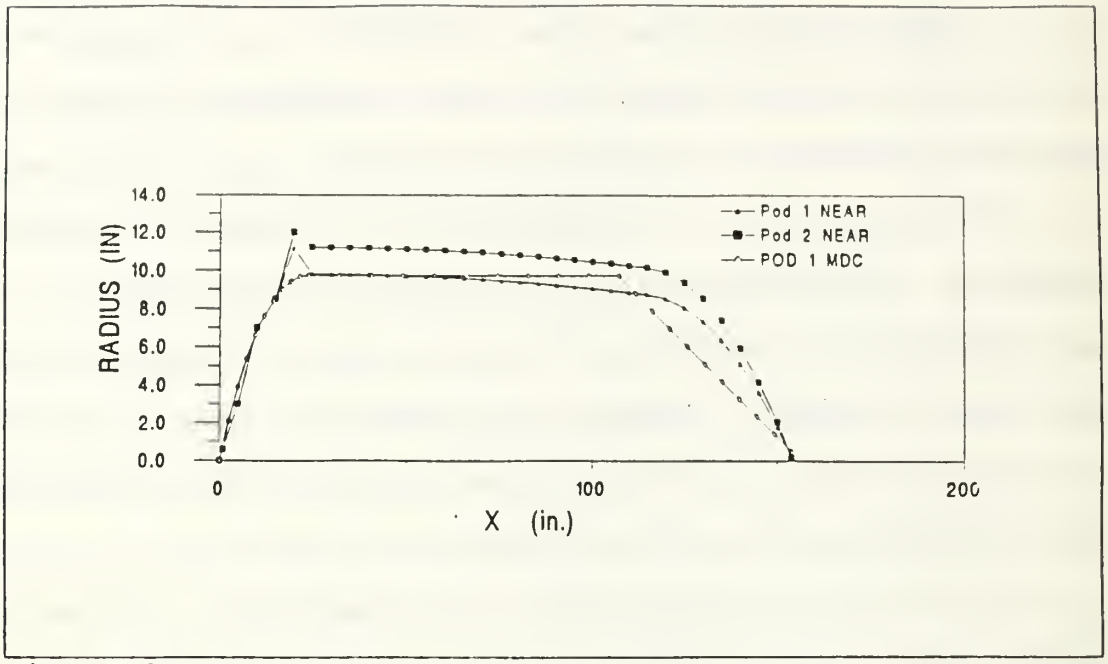

Figure 2 MISDATCOM Pod Shape

```
                                                    THE USAF AUTOMATED MISSILE DATCOM - REV 7/89 -
                                                    AERODYNAMIC METHODS FOR MISSILE CONFIGURATIONS
                                                                CASE INPUTS

FOLLOWING ARE THE CARDS INPUT FOR THIS CASE

CASEID SIMPLE BODY CONFIGURATION FULL LAT
DERIV RAD
DIM IN
DAMP
 $ELTCON NMACH=1.,MACH=0.7,
         REN=4.13E6,
         NALPHA=6.,ALPHA=0.,0.5,1.,2.,3.,4.,BETA=0.5,$
 $REFQ XCG=65.75,$
 $AXIBOD LNOSE=24.,DNOSE=19.5,LCENTR=83.2,DCENTR=19.5,TAIL=0.,
        LAFT=46.6,DAFT=1.0,$
BUILD
PRINT AERO BODY
PRINT GEOM BODY
NEXT CASE

A WARNING A THE REFERENCE AREA IS UNSPECIFIED, DEFAULT VALUE ASSUMED

A WARNING A THE REFERENCE LENGTH IS UNSPECIFIED, DEFAULT VALUE ASSUMED

THE BOUNDARY LAYER IS ASSUMED TO BE TURBULENT OVER ALL COMPONENTS OF THE CONFIGURATION

THE INPUT UNITS ARE IN INCHES, THE SCALE FACTOR IS   1.0000
```

Figure 3 MISDATCOM Input

THE USAF AUTOMATED MISSILE DATCOM * REV 7/89 *
AERODYNAMIC METHODS FOR MISSILE CONFIGURATIONS
SIMPLE BODY CONFIGURATION FULL LAT
BODY ALONE STATIC AERODYNAMIC CHARACTERISTICS

CASE 1
PAGE 4

FLIGHT CONDITIONS								REFERENCE DIMENSIONS				
MACH NUMBER	ALTITUDE	VELOCITY	PRESSURE	TEMPERATURE	REYNOLDS' NUMBER	SIDESLIP ANGLE	ROLL ANGLE	REF. AREA	REF. LENGTH LONG.	REF. LENGTH LAT.	MOMENT REF. CENTER LONG.	MOMENT REF. CENTER VERTICAL
	FT	FT/SEC	LB/IN**2	DEG K	1/FT	DEG	DEG	IN**2	IN	IN	IN	IN
0.70					4.130E+06	-0.50	0.00	298.648	19.500	19.500	65.750	0.000

DERIVATIVES (PER RADIAN)

ALPHA	LONGITUDINAL CN	LONGITUDINAL CM	LONGITUDINAL CA	LATERAL DIRECTIONAL CY	LATERAL DIRECTIONAL CLN	LATERAL DIRECTIONAL CLL	DERIVATIVES LONGITUDINAL CNA	DERIVATIVES LONGITUDINAL CMA	DERIVATIVES LATERAL DIRECTIONAL CYB	DERIVATIVES LATERAL DIRECTIONAL CLNB	DERIVATIVES LATERAL DIRECTIONAL CLLB
0.00	0.000	0.000	0.100	0.004	0.096	0.000	4.526E-01	1.097E+01	-4.566E-01	-1.097E+01	0.000E+00
0.80	0.006	0.153	0.100	0.004	0.096	0.000	4.701E-01	1.096E+01	-4.669E-01	-1.096E+01	0.000E+00
1.00	0.008	0.191	0.100	0.004	0.096	0.000	5.092E-01	1.095E+01	-4.725E-01	-1.096E+01	0.000E+00
2.00	0.017	0.382	0.100	0.004	0.096	0.000	5.609E-01	1.091E+01	-4.998E-01	-1.094E+01	0.000E+00
3.00	0.028	0.572	0.100	0.005	0.095	0.000	6.306E-01	1.085E+01	-5.310E-01	-1.092E+01	0.000E+00
4.00	0.039	0.761	0.099	0.005	0.095	0.000	7.034E-01	1.079E+01	-5.644E-01	-1.088E+01	0.000E+00

ALPHA	CL	CD	CL/CD	X-C.P.
0.00	0.000	0.100	0.000	24.234
0.80	0.005	0.100	0.051	23.566
1.00	0.006	0.100	0.065	23.306
2.00	0.014	0.100	0.139	21.940
3.00	0.023	0.101	0.224	20.590
4.00	0.032	0.102	0.318	19.302

Figure 4 MISDATCOM Output

C. AERODYNAMIC CALCULATION

1. Longitudinal

The aerodynamic coefficients derived from the MISDATCOM were entered into the plant matrix [A] of the longitudinal equations of motion. The initial conditions were applied and time history of the pitch angle, pitch angular velocity, and vertical velocity was found. Figures 5-8 show that the pod assumes a large nose-down, highly divergent pitching motion. This is understandable since there are no control surfaces to make the pod stable. Examination of the roots of the plant matrix [A] indicates an unstable flight vehicle. The pitch angle and pitch rate shown are in the store body coordinate frame.

These results are valid only for the range of linear values of the aerodynamic coefficients. This is approximately up to 10-12 degrees angle-of-attack. Therefore, an estimate of the non-linear behavior of the pod after an AOA of 10 degrees is reached is necessary. Due to the large pitch angular velocity, it is obvious that this limit is reached after only 0.2 seconds. Section V discusses the acceptable time range where these results are valid.

To estimate the non-linear behavior, the dominating terms in the [A]-matrix must be determined. This provides an insight into the possible range of values to substitute into the [A]-matrix. A discussion of a possible approach to this

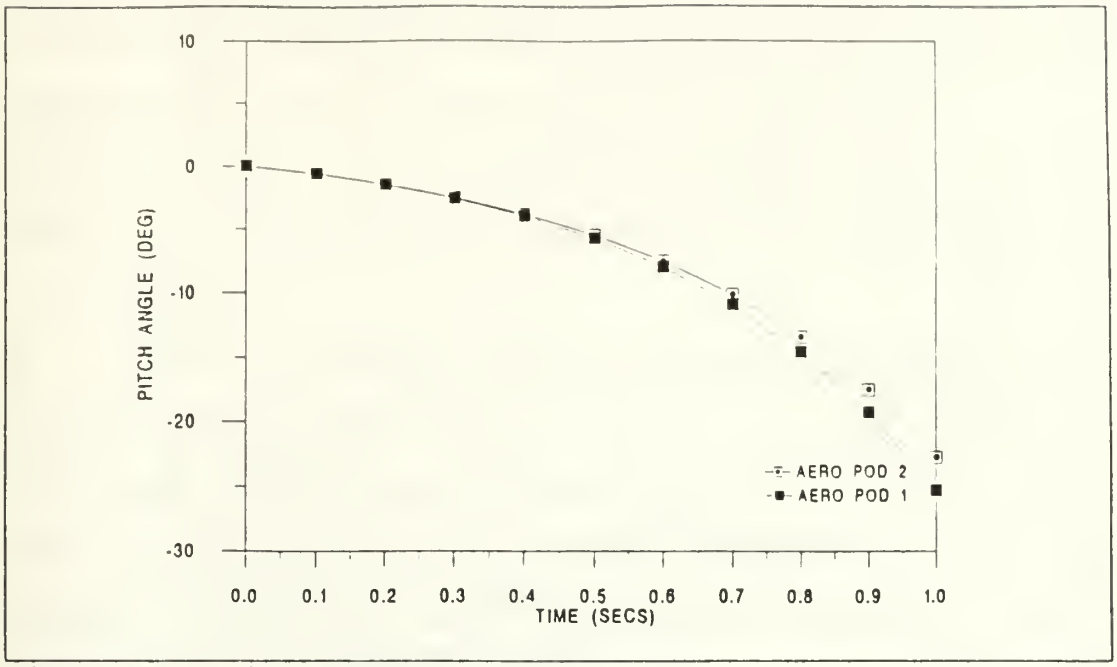

Figure 5 Pitch Angle Response

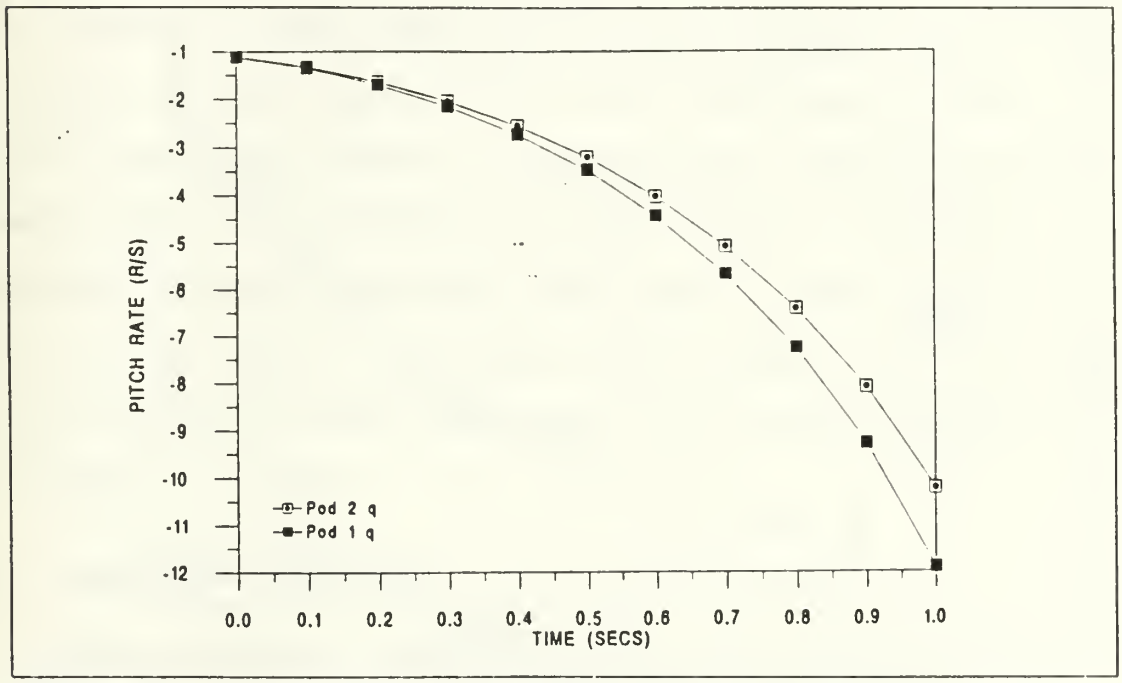

Figure 6 Pitch Rate Response

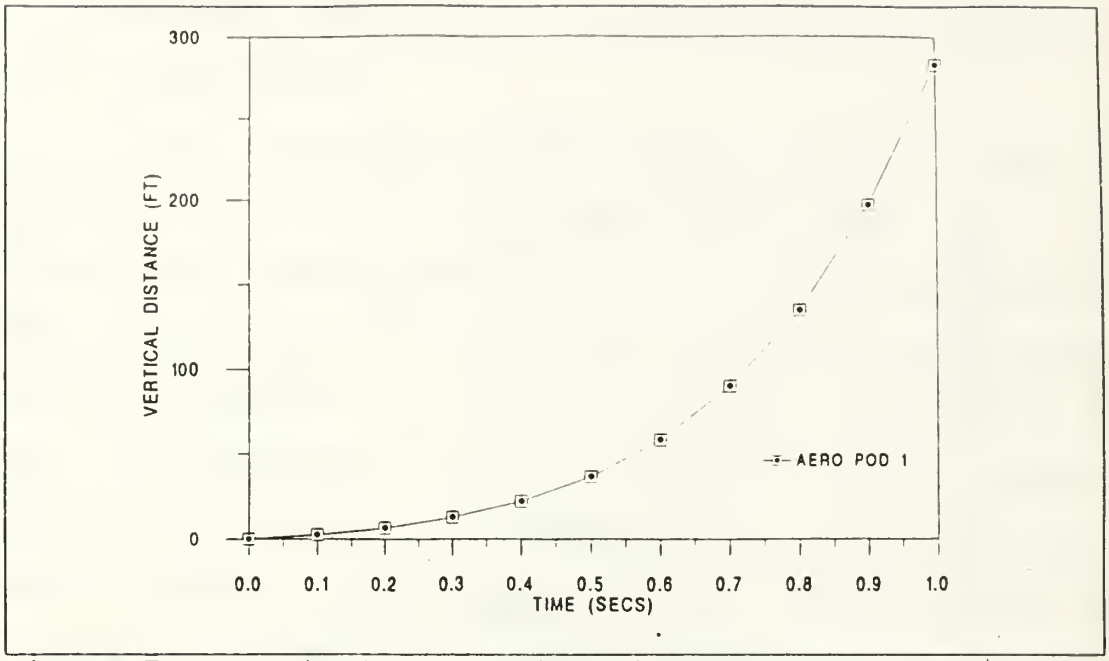

Figure 7 Vertical Separation Distance

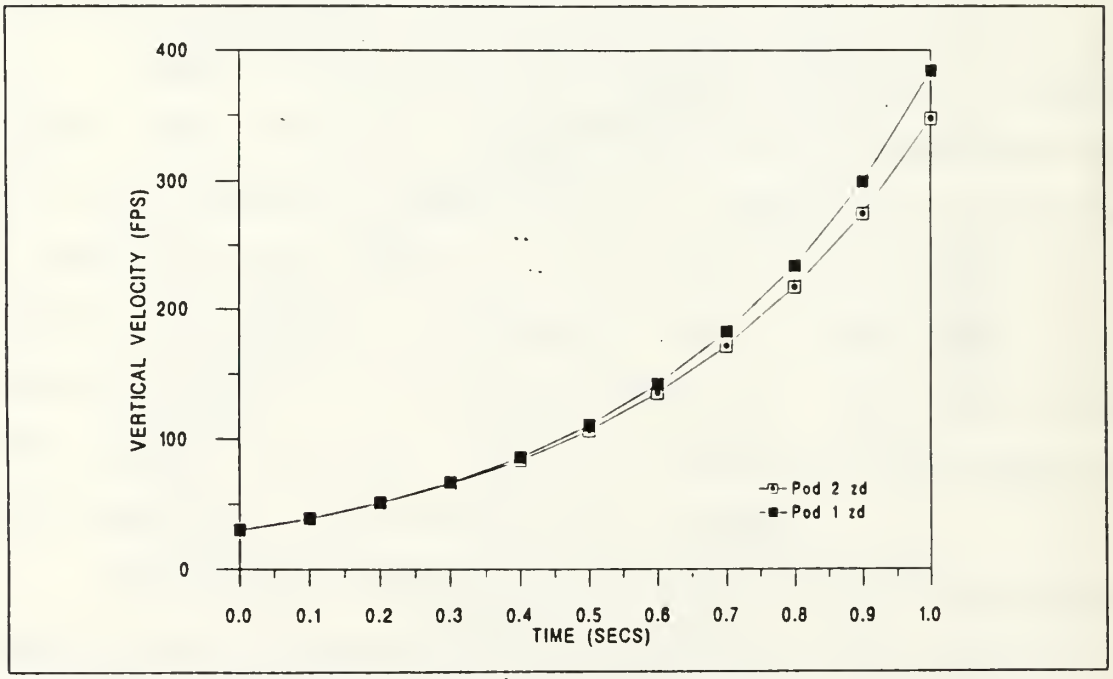

Figure 8 Vertical Velocity

problem is presented in Section V. To completely investigate this area is beyond the scope of the method outlined here. Comparison of the "linear" trajectory obtained here will be made with the trajectory obtained in Section IV, which does take into account the non-linearity of the coefficients.

2. Lateral

Due to the nearly vertical forces and moments provided by the ejection rack during straight and level flight, the free-stream lateral equations of motion will not provide us with any insight into the safe jettison of the shape. However, if the pod were experiencing sideslip, then the sideslip could be entered into the state-space equations as an initial condition. For this pod a sideslip of -0.5 degrees was assumed. The resulting lateral motion is not shown because the main emphasis is on the longitudinal motion. The pod is unstable laterally, also, but the initial movement is small due to the relatively small initial conditions. In addition to the yaw angle and rate, if the ejection rack provided an initial roll rate, such as when the pod is loaded off-center of the bomb rack, then that influence could also be included.

D. PARAMETER VARIATION

The parameter variation due to non-axisymmetry is difficult to handle. Comparison with shapes with known

(experimentally obtained) coefficients might provide some degree of accuracy in predicting more accurate results.

E. PRELIMINARY OBSERVATION

The results of the method in Section II were a vertical velocity of 29.9 feet/sec and an angular velocity of 64.1 deg/sec. The aerodynamic method of Section III begins with a vertical velocity of 29.9 fps, quickly diverging to an extreme value. The pitch rate, q, also diverges quickly. Because the pod is very unstable any linear approximation of its behavior will have strict limits. The coefficients used in this calculation, from the MISDATCOM code, are not valid beyond a fraction of the trajectory. The valid time range of prediction is presented in Section V.

IV. "NEAR" PROGRAM

A. BACKGROUND

A computer prediction method was developed by Nielsen Engineering and Research, Inc., (NEAR) under contract to the United States Air Force. The work was performed during the period 1968 to 1972. The final result is a method for predicting the six degree-of-freedom store separation trajectory at speeds up to the subsonic critical Mach number. After delivery of the program to the Government, many new capabilities were added. The code used for this paper was obtained from the Naval Weapons Center, China Lake, Ca. The program has been widely accepted by industry and government. The code encompasses 9,900 lines of code and thus requires a device with sufficient computer memory for operation. (This also depends upon the program application.)

The aircraft fuselage, separated store body, and adjacent stores are modeled using point sources and sinks. Angle of attack effects are included using a cross-flow model. The aircraft wing and wing pylons are modeled using planar vortex lattice models which include dihedral, camber, and twist of the aircraft wing. Thickness strips are used to model the thickness of the aircraft wing and pylons. [Ref. 10:p. 807]

The capability exists to install multiple sets of wings, fins, or canards, and to use active control surfaces on the store by inputting the control laws into the program. Powered separations may be simulated by inputting the store thrust characteristics.

The NEAR program actually consists of two separate programs: the source program and the trajectory program. Both are described in Section IV.B below.

Alternate separation programs include USTORE and USSAERO codes. USSAERO was developed by F. A. Woodward, of NASA, as a lower-order panel method. USTORE was developed from USSAERO by G. J. van den Broek, of the National Institute for Aeronautics and Systems Technology, Pretoria, South Africa. [Ref. 11:p. 309]

B. THEORY

The three principal tasks in the prediction of a store trajectory are: first, the determination of the nonuniform flow field in the neighborhood of the ejected store; second, the determination of the forces and moments on the store in this flow field; and third, the integration of the equations of motion to determine the store trajectory [Ref. 3].

1. Source Program

The source program is used to represent an axisymmetric body as a distribution of sources along the axis of the body. It provides point source-sink distributions to

represent the fuselage, rack, and store volumes. The program calculates and prints the source strengths and locations. These quantities are then used as input data to the trajectory program.

The source program is used for the generation of an aircraft or pylon model which is then used for the trajectory program. These models are Mach number dependent and thus need to be generated for each test case with different Mach number. For ongoing store separation studies, a good database of aircraft models is required and should be available from appropriate Government facilities. The F/A-18 model was obtained from China Lake along with the program code. This model included pylon stations.

2. Trajectory Program

The trajectory program uses the source-sink distributions from the source program, and additional information to first determine the vorticity distribution which represents the wing-pylon loading including interference of the fuselage, rack, and stores, and then to calculate the store trajectory. See Sections IV.C.3.d.(1) and (2) for descriptions of the vortex lattice method and the panel method.

Once the trajectory program input has been generated for a single flight condition, it is relatively easy for the user to input different stores. The major effort is to obtain

the initial aircraft fuselage, wing, and pylon models for this input.

3. Shape Modeling

a. Aircraft

The aircraft fuselage geometry was modeled by using a Fortran program called NGDELX developed by L. Gleason of the Naval Weapons Center. This program provides the coefficients to the NEAR polynomial representation of equivalent body. The shape is divided into appropriate segments. Radius values for the segment points and maximum radius values are entered. These coefficients are then entered into the source program to generate the source representation of the fuselage. Figure 9 shows the coefficients for the F/A-18 fuselage. Following is the equation used to calculate the coefficients:

$$r_{eq/L} = C_1 + C_7*(C_2*(X/L)^2 + C_3*(X/L)+C_4) + C_5*(X/L)+ C_6*(X/L)^2$$

b. Pylons

The pylons used are modeled the same as in Section IV.C.1.a above. The geometry is used to obtain the NEAR coefficients.

Polynomial Representation of Equivalent Body

$$\frac{r_{eq}}{\ell} = c_1 + c_7\sqrt{c_2\left(\frac{x}{\ell}\right)^2 + c_3\left(\frac{x}{\ell}\right) + c_4} + c_5\left(\frac{x}{\ell}\right) + c_6\left(\frac{x}{\ell}\right)^2$$

x/ℓ	c_1	c_2	c_3	c_4	c_5	c_6	c_7
0.0 to 0.12	-.35763	-1.0	.29259	.12790	0.0	0.0	1.0
0.12 to 0.28	.01978	0.0	0.0	0.0	.06745	0.0	0.0
0.28 to 0.48	.03239	0.0	0.0	0.0	.02318	0.0	0.0
0.48 to 0.542	.88523	-1.0	.82195	.54438	0.0	0.0	-1.0
0.542 to 0.64	-.99071	-1.0	1.280	.68496	0.0	0.0	1.0
0.64 to 1.10	0.0	-.01456	.01863	-.00288	0.0	0.0	1.0

Figure 9 F/A18 NEAR Polynomials

c. Pod or Missile

Again, the procedure in Section IV.C.1.a is used to represent the shape as a set of polynomial coefficients. The NGDELX program is again used to represent the missile shape as an "equivalent body of revolution" (EBR). NGDELX is very easy to use, but, again, only represents axisymmetric shapes.

d. Wing (Lifting Surfaces)

The aircraft wings, missile fins, or any other lifting surfaces are modeled using a vortex lattice method to

represent the loaded wing. The thickness is also modeled using the lattice method.

(1) Vortex Lattice Methods. There are several variations of the vortex lattice method that are presently available and have proven to be very practical and versatile theoretical tools for the aerodynamic analysis and design of planar and non-planar configurations. [Ref. 12 p. 27] The vortex lattice method represents the wing as a planar surface on which a grid of horseshoe vortices is superimposed. The velocities induced by each horseshoe vortex at a specified control point are calculated using the law of Biot-Savart. A summation is performed for all control points on the wing to produce a set of linear algebraic equations for the horseshoe vortex strengths that satisfy the boundary condition of no flow through the wing. The vortex strengths are related to the circulation and the pressure differential between the upper and lower wing surfaces. The pressure differentials are integrated to yield the total forces and moments. [Ref. 13 p.261] For a rigorous introduction to the vortex lattice method, see Reference 13.

(2) Panel Methods. The configuration is modeled by a large number of elementary quadrilateral panels lying either on the actual aircraft surface, or on some mean surface, or on a combination thereof. To each elementary panel, there is attached one or more types of singularity

distributions, such as sources , vortices, and doublets. These singularities are determined by specifying some functional variation across the panel (e.g., constant, linear, quadratic, etc.), whose actual value is set by corresponding strength parameters. These strength parameters are determined by solving the appropriate boundary condition equations. Once the singularity strengths have been determined, the velocity field and the pressure field can be computed. [Ref. 13:p. 258-259]

C. PROCEDURE

1. Source Program

a. Input

The program input consists of the polynomial representation of the equivalent body of revolution (EBR) values obtained in Section IV.B.3.a. The surface of the EBR is approximated by these polynomials, which represent the EBR x,r distribution. The source program is then run with a user-specified finite distribution. The surface obtained from this source distribution can then be compared with the polynomial surface. Additional runs may be required to closely match the surfaces. The aircraft fuselage, pylon(s), and the adjacent store EBR values are input along with two variables, NRAT and PERCR. NRAT is the number of segments which the body will be divided for the specification of the source distribution.

PERCR is the source spacing for each NRAT segment and is input as a fraction of the local body radius of the segment.

Adjacent stores are included in the aircraft source input. In this way it becomes part of the aircraft configuration. The separated store is not input to the source program since the trajectory program calls the source program during its execution to model the store. this is due to the fact the store changes position during the program run and the sources/sinks will change values. Figure 10 lists a sample format for the source program input.

```
FILE: 2-F18SOU T        A1


1f-18 AIRCRAFT
    1
    1
F-18  AIRCRAFT
    6    0.70
 0 0 0 0 0 0 0 0 0 0 0 0 0 0 0 0 0 0 0 0 0
0.12        0.28       0.48       0.542      0.64       1.0
-.35763    -1.0        0.29259    0.12790    0.0        0.0        1.0
0.01978     0.0        0.0        0.0        0.06745    0.0        0.0
0.03239     0.0        0.0        0.0        0.02318    0.0        0.0
0.88523    -1.0        0.82195    0.54438    0.0        0.0       -1.0
-.99071    -1.0        1.28       0.68496    0.0        0.0        1.0
0.0        -0.01456    0.01863   -.00288     0.0        0.0        1.0
0.001       1.1        0.6400     0.         1.         0.02       0.0555
    6
0.10046    0.15525    0.28311    0.37443    0.97717    1.0
0.6        0.8        1.0        1.2        .8         .8
```

Figure 10 Source Program Input

b. Output

The source program output is used as input to the trajectory program. However, it is not directly read into the trajectory input and must be entered via keyboard. The form of the output is shown as a partial output in Figure 11. Source locations and strengths are listed.

```
F-16  AIRCRAFT


X/L OF END POINT OF EACH SECTION OF BODY


 SECTION      1         2         3         4         5         6
 X/L       0.12000   0.28000   0.48000   0.54200   0.64000   1.00000


COEFFICIENTS OF POLYNOMIAL DESCRIBING EACH SECTION

  SECTION      C1        C2        C3        C4        C5        C6        C7
     1     -0.95763  -1.00000   0.29259   0.12790   0.00000   0.00000   1.00000
     2      0.01978   0.00000   0.00000   0.00000   0.06745   0.00000   0.00000
     3      0.03239   0.00000   0.00000   0.00000   0.02310   0.00000   0.00000
     4      0.08523  -1.00000   0.82195   0.54438   0.00000   0.00000  -1.00000
     5     -0.99071  -1.00000   1.28000   0.68496   0.00000   0.00000   1.00000
     6      0.00000  -0.01456   0.01863  -0.00288   0.00000   0.00000   1.00000


FIRST SOURCE AT X/L= 0.00100
LAST SOURCE AT X/L =  1.10000

FROM   0.00100  TO   0.10044  SOURCE SPACING IS   0.60000  TIMES LOCAL RADIUS
FROM   0.10044  TO   0.15525  SOURCE SPACING IS   0.80000  TIMES LOCAL RADIUS
FROM   0.15525  TO   0.28311  SOURCE SPACING IS   1.00000  TIMES LOCAL RADIUS
FROM   0.28311  TO   0.37443  SOURCE SPACING IS   1.20000  TIMES LOCAL RADIUS
FROM   0.37443  TO   0.97717  SOURCE SPACING IS   0.80000  TIMES LOCAL RADIUS
FROM   0.97717  TO   1.00000  SOURCE SPACING IS   0.60000  TIMES LOCAL RADIUS


FOR THIS CASE THERE ARE  74 SOURCES


SOURCE LOCATIONS AND BODY RADIUS AND SURFACE SLOPE AT THESE LOCATIONS

  X/L      0.00100   0.00118   0.00138   0.00162   0.00190   0.00224   0.00263
  R/L      0.00041   0.00048   0.00056   0.00066   0.00077   0.00091   0.00106
  DR/DX    0.40581   0.40524   0.40457   0.40379   0.40287   0.40180   0.40054

  X/L      0.00308   0.00361   0.00424   0.00497   0.00583   0.00682   0.00799
  R/L      0.00125   0.00146   0.00171   0.00199   0.00233   0.00272   0.00317
  DR/DX    0.39906   0.39754   0.39533   0.39298   0.39024   0.38705   0.38334

  X/L      0.00934   0.01092   0.01275   0.01488   0.01733   0.02017   0.02342
  R/L      0.00368   0.00428   0.00496   0.00573   0.00661   0.00760   0.00871
  DR/DX    0.37904   0.37406   0.36830   0.36167   0.35405   0.34534   0.33540

  X/L      0.02716   0.03142   0.03625   0.04172   0.04787   0.05474   0.06235
  R/L      0.00994   0.01129   0.01277   0.01435   0.01602   0.01776   0.01954
  DR/DX    0.32418   0.31139   0.29709   0.28112   0.26341   0.24390   0.22257

  X/L      0.07072   0.07988   0.08971   0.10025   0.11139   0.12693   0.14312
  R/L      0.02138   0.02301   0.02460   0.02601   0.02719   0.02834   0.02943
  DR/DX    0.19944   0.17457   0.14805   0.12003   0.09069   0.06745   0.06745

  X/L      0.15993   0.18176   0.20464   0.22863   0.25377   0.28012   0.30780
  R/L      0.03057   0.03204   0.03338   0.03520   0.03690   0.03838   0.03953
  DR/DX    0.06748   0.06748   0.06745   0.06745   0.06745   0.02310   0.02310

  X/L      0.34176   0.37630   0.39979   0.42359   0.44771   0.47214   0.49690
  R/L      0.04031   0.04111   0.04166   0.04221   0.04277   0.04333   0.04505
  DR/DX    0.02310   0.02310   0.02310   0.02310   0.02310   0.02310   0.10227

  X/L      0.52264   0.55011   0.57961   0.61032   0.64179   0.67349   0.70511
  R/L      0.04808   0.05163   0.05376   0.05500   0.05549   0.05534   0.05493
  DR/DX    0.13330   0.08624   0.05702   0.02838  -0.00053  -0.00887  -0.01732

  X/L      0.73649   0.76749   0.79794   0.82771   0.85665   0.88460   0.91144
```

Figure 11 Source Program Output

2. Trajectory Program

The trajectory program uses the output of the source program, and the input of the wing configuration and pylons, along with store information to calculate the trajectory of the separated store. It is not the intent of this report to fully explain the aircraft modeling details of the program. The assumption is made that the appropriate aircraft model is available for the correct flight condition and configuration. The applicable store inputs to the program are discussed and the resulting trajectory examined. Nielson contains a thorough description of the theory and input of the aircraft model in Reference 3.

a. Input

The example input to the trajectory program was 1064 lines in size. The store data entry begins at approximately 980 lines, depending upon aircraft input. The store input will vary according to the physical configuration of the store. For the example separation, Input Items 35-43 and 48-51 were used to input store physical data. The ejector information was input in Items 44A-47. This is where the fifth-order polynomial representation of the ejector force was used. Data concerning initial and final times, and integration step sizes were entered in Input Item 72. The correct input form of the above data is contained in the NEAR code users manual [Ref. 14] and is not presented here.

b. Output

The output of the trajectory program is dependent upon the input conditions, i.e., the number of stores, number of store segments, and number of integration steps, etc. The example case output is 4,524 lines. The first 1,840 lines of output are aircraft-specific output, such as the source and vorticity information.

The last 2,650 lines of code contain the trajectory data. The ejector force data is repeated as is the store shape data, reference dimensions and inertial characteristics.

Proceeding the ejector data, a data block is presented for each time integration step. This data block contains the parameters which describe the store displacement, velocity, and acceleration during the separation. A partial sample output of this section of the output file is included in Figure 12. Plotting routines can be developed to facilitate data analysis of the simulation but have not been developed for this study. The following are short descriptions of some of these parameters. A comparison with the results of the method of Section III follows in Section IV.D.

The force and moment coefficients are listed by their individual contributions. The effects of buoyancy, slender body theory, crossflow, and empennage are totaled to give an effective C_N, C_Y, C_{lm}, and C_{ln}.

```
0000 EJECTOR DATA

      EFOOT  MEPOLY(I)      XE(I)          THETAE(I)      STROKE(I)
        1        1         -1.0999           0.00          999.0000

             TRNDI(I,1)     TRNDI(I,2)     TRNDI(I,3)     TRNDI(I,4)     TRNDI(I,5)
             0.0000E-01     0.0000E+00     0.0000E+00     0.0000E+00     0.0000E+00

***** TIME  IS THE INDEPENDENT EJECTOR VARIABLE *****

      EFOOT  MEPOLY(I)      XE(I)          THETAE(I)      STROKE(I)
        0        1          0.1950           0.00          999.0000

             TRNDI(I,1)     TRNDI(I,2)     TRNDI(I,3)     TRNDI(I,4)     TRNDI(I,5)
             0.0000E-01     0.0000E+00     0.0000E+00     0.0000E+00     0.0000E+00

***** TIME  IS THE INDEPENDENT EJECTOR VARIABLE *****

   COEFFICIENTS OF NTH DEGREE POLYNOMINAL

    EFOOT       I          C1             C2             C3             C4             C5             C6

      1         1     0.2003E+03    -0.6000E+06     0.1007E+07    -0.1004E+11     0.2345E+12    -0.1704E+13

      2         2     0.2003E+03    -0.6000E+06     0.1007E+07    -0.1004E+11     0.2345E+12    -0.1704E+13
   STORE NUMBER    1 IS THE STORE EJECTED

      ADDITIONAL INPUT FOR THIS STORE
         STORE MASS =    11.500 SLUGS
         MOMENTS AND PRODUCTS OF INERTIA, SLUG - SQ FT
            IXX =         9.00
            IYY =        92.00
            IZZ =        92.00
            IYZ =         0.00
            IXZ =         0.00
            IXY =         0.00

         STORE MOMENT CENTER IS   -9.400 FEET BEHIND NOSE
         STORE REFERENCE AREA IS        2.695 SQ.FT.
         STORE REFERENCE LENGTH IS      1.655 FT.

         STORE CENTER OF GRAVITY OFFSET FROM MOMENT CENTER, FEET
            XBAR =  0.00000
            YBAR =  0.00000
            ZBAR =  0.00000
         POLYNOMIALS SPECIFYING COMPRESSIBLE STORE SHAPE
            X/L OF END OF EACH SECTION
               SECTION      X/L          TYPE FIT IS = NO. I = POLYI
                  1       0.01350                0
                  2       0.06500                0
                  3       0.09750                0
                  4       0.15600                0
                  5       0.79470                0
                  6       1.00000                0
               COEFFICIENTS OF POLYNOMIALS DESCRIBING EACH SECTION
                  SECTION     C1        C2        C3        C4        C5        C6        C7
                     1      0.00000   0.00000   0.00000   0.00000   0.00000   0.00000   0.00000
                     2      0.01219  -1.00000   0.11006  -0.00715   0.00000   0.00000   1.00000
                     3     -0.00179  -1.00000   0.19506  -0.00402   0.00000   0.00000   1.00000
                     4      0.01441  -1.00000   0.27010  -0.01548   0.00000   0.00000   1.00000
```

Figure 12 Trajectory Program Partial Output

```
FILE: TEX12    TX       A1

     TIME =     0.1150  TIMEP =     1.0000  ETIME =     0.0500
1    TIME = 0.11500 SECONDS

     FORCE AND MOMENT COEFFICIENTS (REF. AREA =  2.010 FT**2  --   REF. LENGTH = 1.633 FT.)
                          CN         CY         CLM        CLN        CLL
       BUOYANCY       -0.50107    0.01059    0.09415   -0.05126
       SLENDER BODY    1.76770   -0.02679    0.96167   -0.10729
       CROSSFLOW       0.10901   -0.00241   -0.69002    0.00007
       EMPENNAGE 1     0.00000    0.00000    0.00000    0.00000    0.00000
       TOTAL           1.37506   -0.01861    0.35990   -0.22965    0.00000

     LOCATION OF STORE 101 FUSELAGE COORDINATE SYSTEM, DIMENSIONS OF FEET
                 RELATIVE TO FUSELAGE NOSE          RELATIVE TO INITIAL POSITION
                    XF         YF         ZF          DEL XF     DEL YF     DEL ZF
          NOSE  -27.96376 -11.19107    6.11918       -0.00228   -0.00107    4.11958
          XMOM  -33.86922 -11.19010    8.19066       -0.01125   -0.00010    3.52504
          BASE  -40.60001 -11.18601    8.95237        0.00309    0.00119    3.67171

     TRANSLATIONAL VELOCITIES AND ACCELERATIONS OF STORE IN FUSELAGE COORDINATE SYSTEM
          RELATIVE TO FUSELAGE MOTION
               DXF        DYF        DZF       D2XF       D2YF       D2ZF
            -0.16504   -0.00110   33.17662   -1.20077   -0.00393   21.05520

     ROTATIONAL VELOCITIES AND ACCELERATIONS OF STORE IN STORE COORDINATE SYSTEM
                P          Q          R        PDOT       QDOT       RDOT
            0.00023   -3.01056   -0.00260    0.00000    0.64850   -0.01762

     STORE ANGULAR ORIENTATION IN FUSELAGE COORDINATE SYSTEM AND RATES OF CHANGE OF THESE ANGLES
          ANGLES IN DEGREES, RATES OF CHANGE IN RADIANS PER SECOND
               PSI       THETA       PHI       DPSI      DTHETA      DPHI
            -0.01023   -0.71236    0.00266   -0.00275   -3.01056    0.00069

     TIME =     0.1350  TIMEP =     1.0000  ETIME =     0.0500
1    TIME = 0.13500 SECONDS

     FORCE AND MOMENT COEFFICIENTS (REF. AREA =  0.095 FT**2  --   REF. LENGTH = 3.633 FT.)
                          CN         CY         CLM        CLN        CLL
       BUOYANCY       -0.04070    0.00900    0.10575   -0.04700
       SLENDER BODY    1.74653   -0.02450    0.05120   -0.17050
       CROSSFLOW       0.10519   -0.00220   -0.68300    0.00010
       EMPENNAGE 1     0.00000    0.00000    0.00000    0.00000    0.00000
       TOTAL           1.56300   -0.01745    0.27310   -0.21036    0.00000

     LOCATION OF STORE IN FUSELAGE COORDINATE SYSTEM, DIMENSIONS OF FEET
                 RELATIVE TO FUSELAGE NOSE          RELATIVE TO INITIAL POSITION
                    XF         YF         ZF          DEL XF     DEL YF     DEL ZF
          NOSE  -27.98697 -11.19143    8.09330       -0.10550   -0.00141    4.94178
          XMOM  -33.26077 -11.19010    8.06054       -0.01401   -0.00012    4.19574
          BASE  -40.07729 -11.18068    4.47720        0.10666    0.00150    3.19660

     TRANSLATIONAL VELOCITIES AND ACCELERATIONS OF STORE IN FUSELAGE COORDINATE SYSTEM
          RELATIVE TO FUSELAGE MOTION
               DXF        DYF        DZF       D2XF       D2YF       D2ZF
            -0.10555   -0.00155   33.01365   -1.20240   -0.00305   21.05107

     ROTATIONAL VELOCITIES AND ACCELERATIONS OF STORE IN STORE COORDINATE SYSTEM
                P          Q          R        PDOT       QDOT       RDOT
            0.00010   -3.03701   -0.00255    0.00000    0.65665   -0.01653

     STORE ANGULAR ORIENTATION IN FUSELAGE COORDINATE SYSTEM AND RATES OF CHANGE OF THESE ANGLES
          ANGLES IN DEGREES, RATES OF CHANGE IN RADIANS PER SECOND
               PSI       THETA       PHI       DPSI      DTHETA      DPHI
            -0.01360   -10.03251    0.00302   -0.00311   -3.03701    0.00083


     TIME =     0.1550  TIMEP =     1.0000  ETIME =     0.0500
     TIME = 0.17500 SECONDS

     FORCE AND MOMENT COEFFICIENTS (REF. AREA =  0.090 FT**2  --   REF. LENGTH = 3.833 FT.)
                          CN         CY         CLN        CLM        CLL
       BUOYANCY       -0.00060    0.00755    0.10035   -0.04460
```

Figure 13 Trajectory Output (Cont)

The ejector force and moment components are listed. The vertical force history matches the force profile from Section II very closely. The store's nose, inertial reference center, and the base position in the fuselage coordinate system is listed. The separation distance from the initial position is also listed as output. Plots of these parameters will indicate the miss distance of the shape from the wing. The store translational and rotational velocities are output in both the store's reference frame and the fuselage reference frame.

V. RESULTS AND COMPARISONS

A. EJECTOR FORCES AND MOMENTS

1. Vertical Velocity

The predicted end-of-stroke vertical velocity from the hand-calculation was 29.9 fps, comparing with the NEAR code results of 30.84. This is a 3% difference. The predicted value from the ejector graph of Reference 4 yields 24.5 fps. The ejector graph is representative of the average store used in the Naval inventory, which more than likely would have control surfaces for stability reasons. These surfaces would also provide aerodynamic damping which could be the source of the discrepancy.

2. Pitch Rate Q

The predicted pitch rate, q, of 1.12 radians/second matches well with the NEAR end-of-stroke q of 1.08 radians/second. For most applications, this correlation of 4% should have sufficient accuracy.

B. TRAJECTORY COMPARISON

The main consideration in determining the accuracy of these trajectory methods is the safe separation (or jettison) of the pod. Vertical distance and pitch attitude are indications of the pod separation while velocity and angular velocity are indications of the store loads. Therefore,

criteria for judging the correlation between the linear method and the NEAR code must be based on the practical standpoint of a reasonable assumption of safe separation. The individual parameters are addressed below. For determining the valid time range of the aerodynamic prediction method, the NEAR code was used as reference.

1. Vertical Separation Z

Vertical distance z in the linear method is derived from the vertical velocity term. Therefore the error (deviation from NEAR results) will be slightly less due to the integration effects. However, given the initial vertical velocity, the NEAR code predicts a five foot separation. The error limit must be set as an acceptable variation of this distance. Based upon practical knowledge of store separation, a 20% error limit was set. Figure 14 compares the linear aerodynamic method results comparison with the NEAR results in the amplified time region of the first 0.2 seconds.

2. Pitch Angle

Since the pitch angle is used solely for determining the safe separation and is not used for more accurate applications, like rocket engine ignition, the effect of an error in pitch will vary as the sine of the angle deviation. This could result in an error, due to rotation about the center of gravity, of an order of 7.2 feet times the sine of the error angle. The pitch angle error must be fairly small

initially, but can grow as time increases due to increased separation distance and its decreasing effect. Therefore, a conservative error limit is set for 0.1 sec. At 0.1 seconds, the NEAR pod has rotated 4.5 degrees. A 30% error would give a vertical error of 0.2 feet, which is approximately 10% of the actual separation. Figure 15 shows a comparison of the linear method with the NEAR results. Figure 16 provides the error between the methods as a function of time.

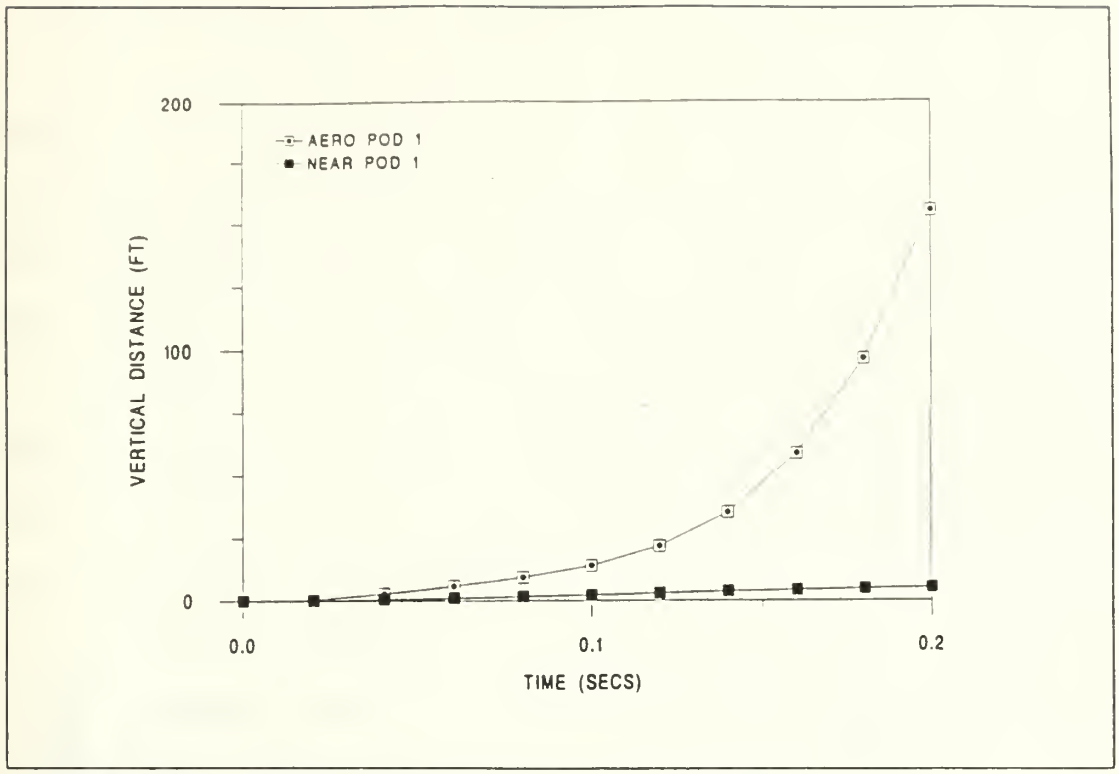

Figure 14 Vertical Separation Distance

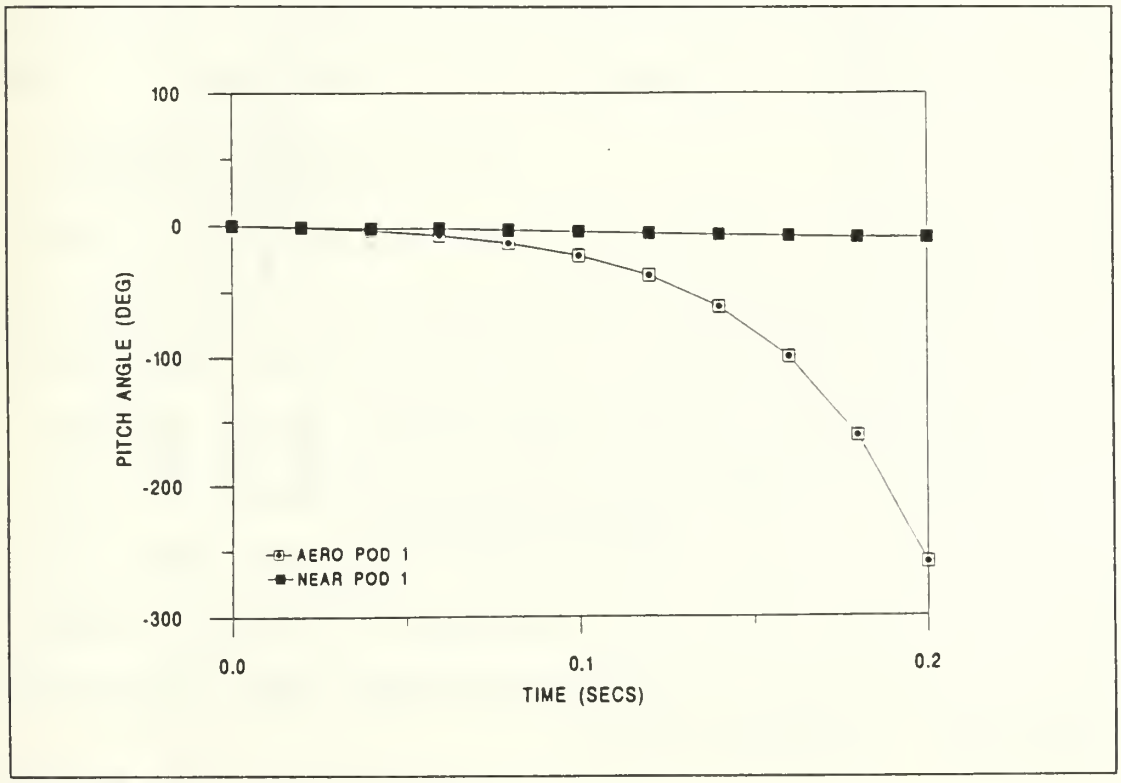

Figure 15 Pitch Angle

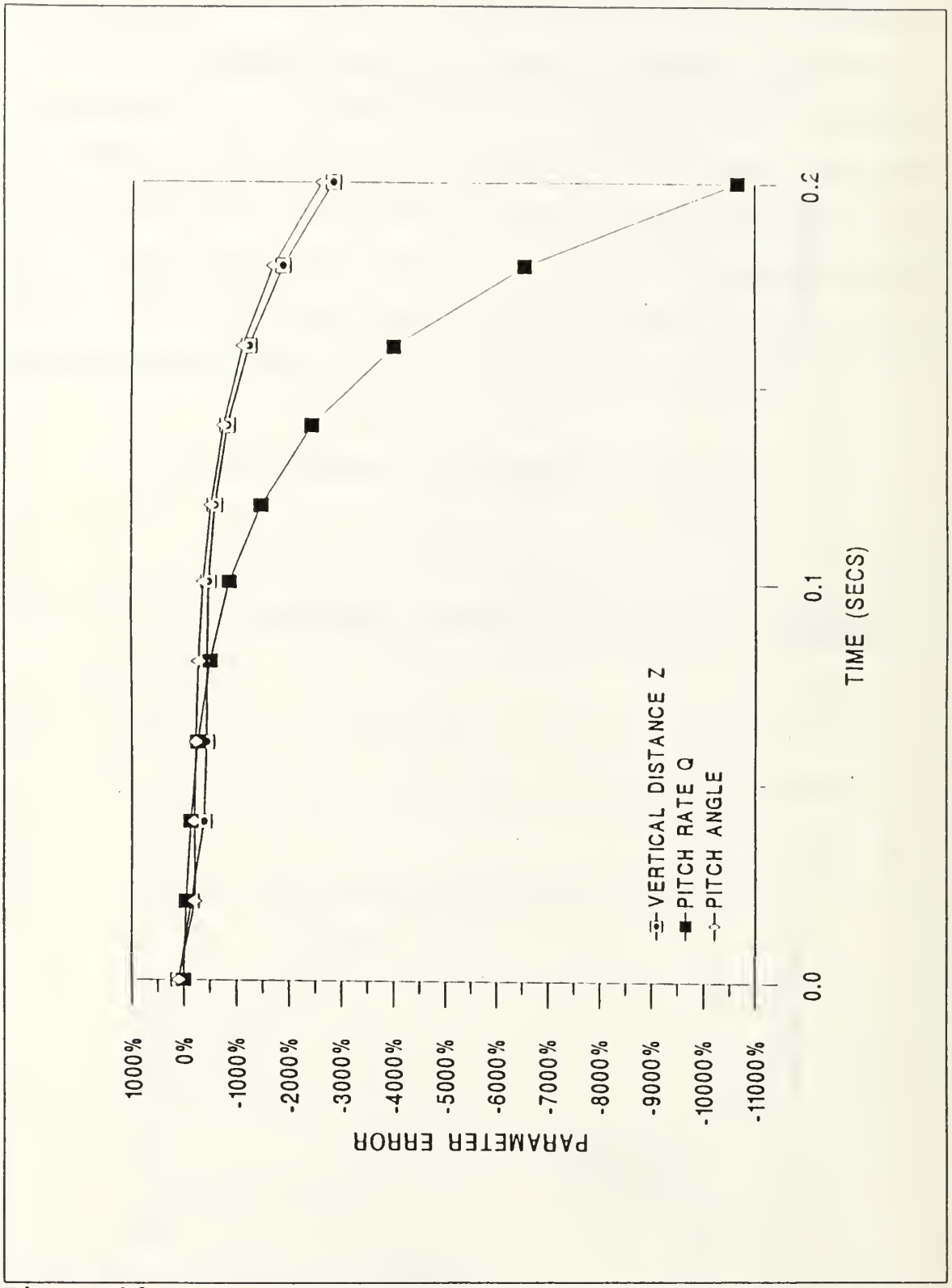

Figure 16 Parameter Error

3. Pitch Rate

The required accuracy for pitch rate will be determined by its application. For instance, navigational considerations will require quite accurate predictions of the angular loading of its components. However, for this case, there is not a requirement of this kind. The divergent nature of the pitch rate from the linear aerodynamic model does not present a problem for this case, beyond the fact that the pitch angle follows this trend. Therefore, an error limit is not placed upon the pitch rate.

4. Vertical Velocity

Vertical velocity is divergent and represents the lack of aerodynamic damping in the linear model. Therefore, it does not provide meaningful information beyond the phase relationship with the vertical separation distance. For this reason, an error limit is not placed upon the velocity.

C. AUGMENTED AEROPREDICTION

Due to the limited valid time limits on the aerodynamic method, an alternative approach was investigated. Obviously, the non-linear operating region is reached very quickly. The two dominant terms of the A-matrix are the damping terms, C_{Mq} and $C_{M\dot{\alpha}}$. The unstable pod is shown from the NEAR code to quickly reach a somewhat steady-state value of pitch rate as it tumbles. An effort was made to calculate a new (and valid) value of C_{Mq}. This approach modeled the tumbling store as a

cylinder of constant radius. Using a value of C_d=1.0, and the end-of-stroke pitch rate of 1.12 radians/second, new values of damping coefficients were calculated.

1. C_{Mq}- **Coefficient**

The new pitch damping coefficient of -.1054 was used versus the MISDATCOM value of -.04. This is an obvious improvement and also realistic since the pod will definitely experience aerodynamic damping, due to pitch rate, that would not have been predicted by MISDATCOM.

2. $C_{M\dot{\alpha}}$- **Coefficient**

The value of the aerodynamic damping effects of change in angle of attack, $C_{M\dot{\alpha}}$, was combined with C_{Mq} in the MISDATCOM output. Therefore, the valid value of $C_{M\dot{\alpha}}$ is unclear. For this model of a rotating pod, it was assumed that $C_{M\dot{\alpha}}$ would have minimal effect on the damping and a value of 0.0 was assigned.

3. **Trajectory Prediction**

The predicted parameters using the above coefficients are contained in Figures 17, 18 and 19. As shown in the figures, there is considerable improvement in the correlation with the NEAR trajectories for pitch angle and pitch rate. The more realistic value for C_{Mq} obviously improves the results. The time range of validity for these two parameters is now estimated to be 1.0 seconds. However, the most important parameter, vertical separation distance, is still

outside of reasonable accuracy limits. Therefore, the augmented plant matrix method is still unusable for complete trajectory prediction. Figure 20 shows the parameter error for the augmented system.

Although there is substantial correspondence in the partial comparison between the NEAR results and these results, there are not enough data points to substantiate this method. Further work using different shapes need to be done.

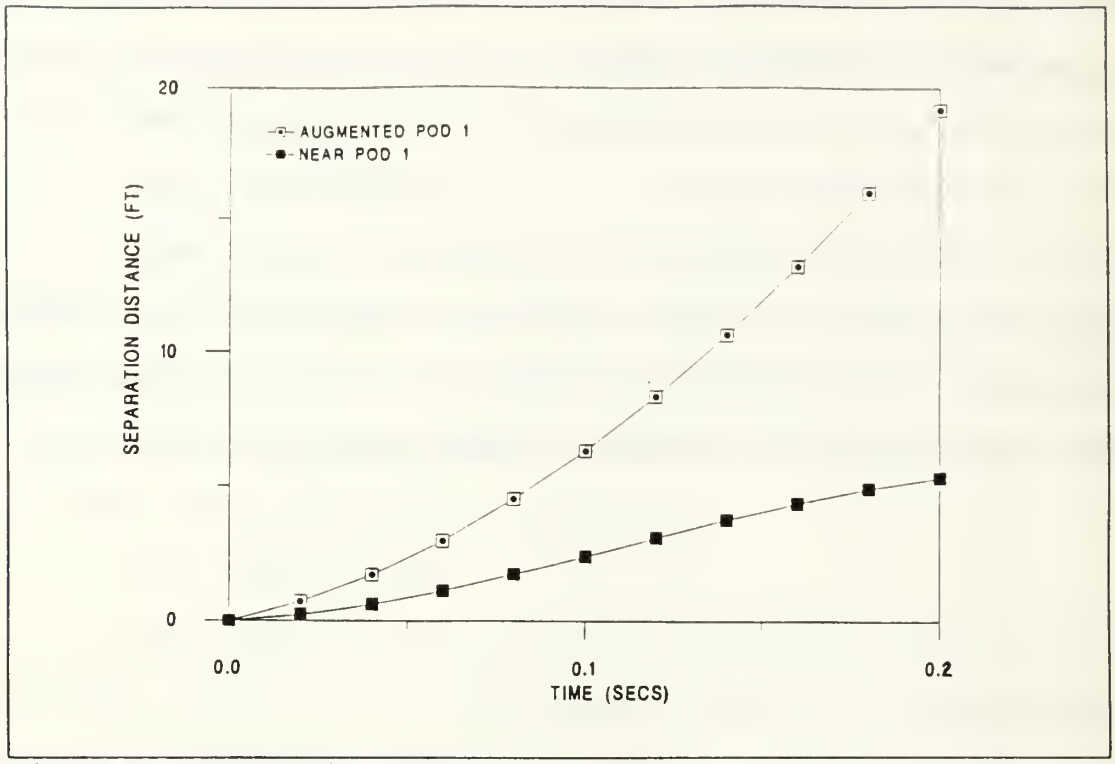

Figure 17 Vertical Separation Distance (Augmented)

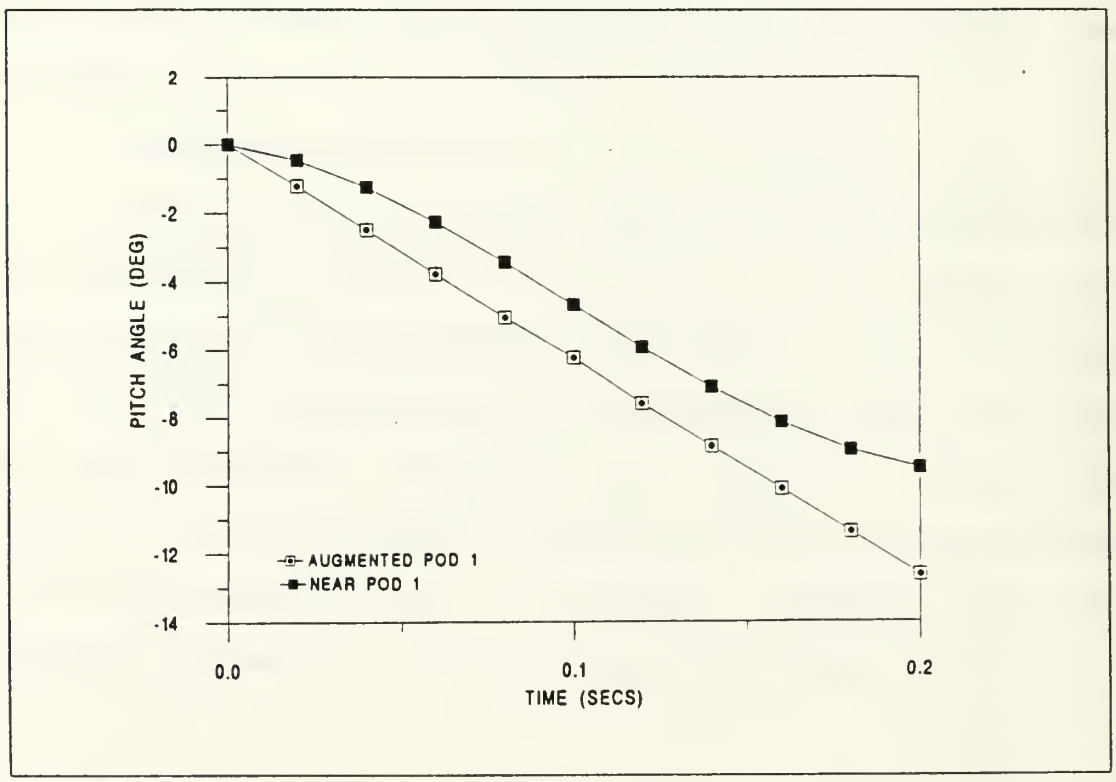

Figure 18 Pitch Angle (Augmented)

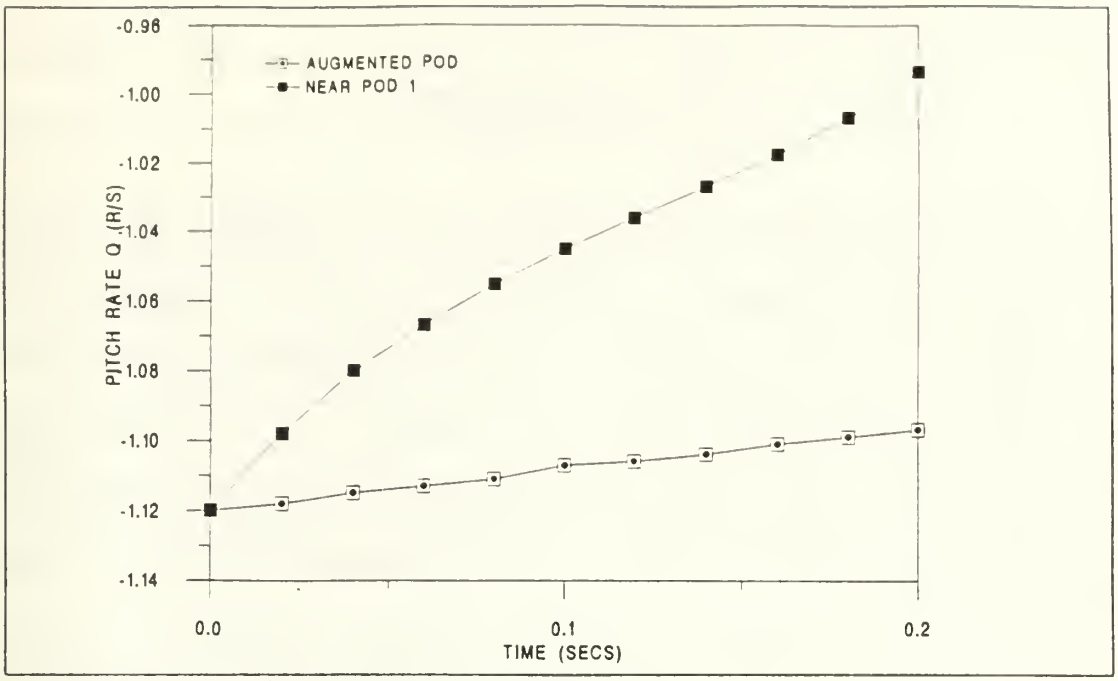

Figure 19 Pitch Rate (Augmented)

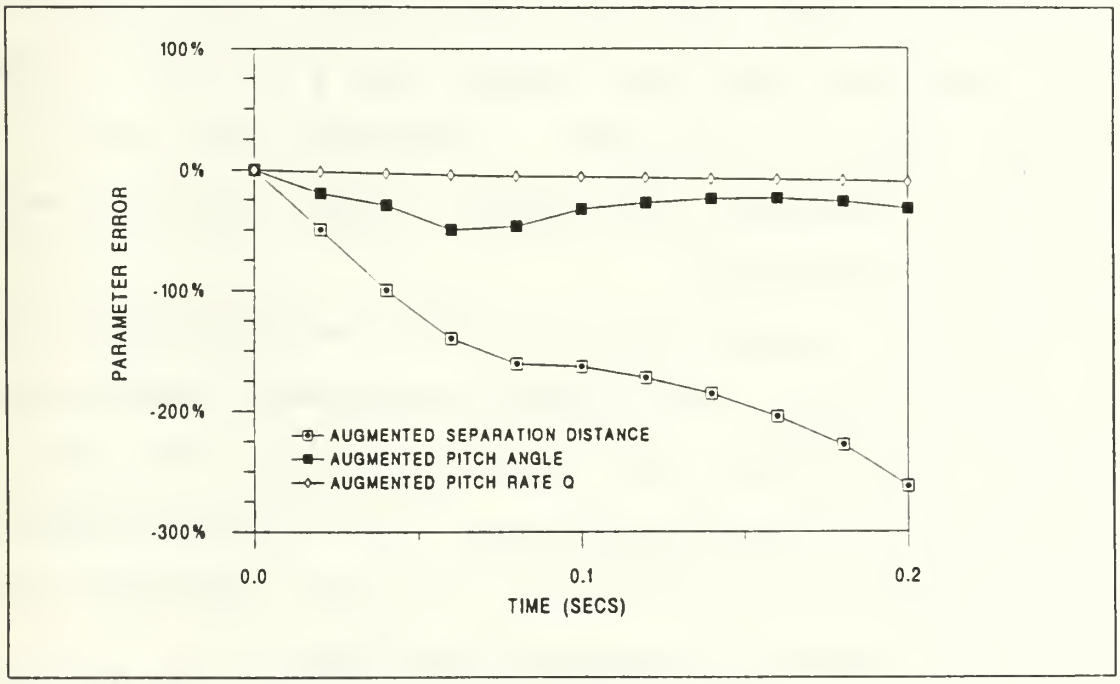

Figure 20 Parameter Error (Augmented)

VI. CONCLUSIONS

In the preliminary design application, MISDATCOM provides an easy-to-use method to predict moderately accurate store aerodynamic characteristics. These aerodynamic coefficients can be used to model the store dynamics for design work. However, their use in the linearized equations of motion for an externally ejected store trajectory prediction is highly limited.

Comparisons with the Nielson Engineering and Research (NEAR) code show that trajectory values are outside of reasonable accuracy limits for use in store separations. The store separation vertical distance and pitch angle values diverged within 0.1 seconds. Therefore, the use of the linearized equations of motion cannot provide useful trajectory information.

However, a modification to these coefficients to more accurately reflect the existing aerodynamic damping does provide correlations with the NEAR code of within 30% for pitch angle and 10% for pitch rate. Use of these "augmented" linear equations of motion for attitude prediction shows sufficient accuracy for many applications.

The NEAR code is widely used for ejected store trajectory prediction in the aviation field. Its use for safe separation

investigation should be considered as standard for obtaining accurate results. The cost of the Nielson code in both engineering time and computational time increases with the level of information produced, but the need for safe separation accuracy, aerodynamic load distributions, and vortex-induced effects make the extra effort justified.

For limited applications requiring less accuracy, the augmented linear equations of motion can provide some information for the initial trajectory movement. A potential application would be the investigation of the effects of small weight or inertial modifications to existing stores.

APPENDIX A

A. POD CHARACTERISTICS

The pod in question was an ALE-29B pod modified to accommodate the SUU-53 chaff dispenser and associated equipment. The ALE-29 pod was flight approved by the Aircraft Configuration Control Board (ACCB) document #75-004. It was originally an ALE-2 pod. No significant aerodynamic changes have been made to the pod.

The pod physical characteristics are listed in Table 1.

TABLE 1 POD CHARACTERISTICS

Length	153.8 inches
Radius -minimum	9.75 inches
-maximum	11.20 inches
CG location -empty	62.4 inches from nose
-full	65.4 inches
Weight -empty	326 lbs
-full	371 lbs
Moment of Inertias	
-Ixx	300 $lb\text{-}ft^2$
-Iyy	1675 $lb\text{-}ft^2$
-Izz	1675 $lb\text{-}ft^2$

APPENDIX B

A. FORCE EQUATIONS

$$\Sigma F = M*\dot{V} = d/dt(M*V) = \dot{G}$$

Separating variables:

$$\Sigma F_x = \dot{G}_x \qquad \Sigma F_y = \dot{G}_y \qquad \Sigma F_z = \dot{G}_z$$

Assuming $\Sigma F_{x,y} = 0$,

Integrating the remaining equation,

$$\int \Sigma F_z \, dt = G_2 - G_1 = (M*V_z)_2 - (M*V_z)_1$$

Assuming straight and level flight, $V_{z1} = 0$ yields:

$$\int \Sigma F_z \, dt = M*\Delta V_z = M*V_z$$

Integrating the ejector force polynomial yields a total impulse of 345 lb_f-secs. Substituting (wt=371 lb),

$$345 \ lb_{f\text{-secs}} = 371 \ lb_m * V_z$$

$$V_z = 1.1773 \ (lb_f\text{-sec}/lb_m) * 32.174 \ (lb_m\text{-ft}/lb_f\text{-sec}^2)$$

$$V_z = 29.9 \text{ fps}$$

B. MOMENT EQUATIONS

$$\Sigma M_o = r \times \Sigma F = r \times M*\dot{V} = d/dt(r \times M*V) = \dot{H}_o$$

where H_o is the angular momentum about pt O. Integrating the moments,

$$\int \Sigma M_o \, dt = \dot{H} + r \times H$$

Separating the component equations yields,

$$\Sigma M_x = I_{xx}*\dot{\omega}_x - (I_{yy} - I_{zz})*\omega_y*\omega_z$$
$$\Sigma M_y = I_{yy}*\dot{\omega}_y - (I_{zz} - I_{xx})*\omega_z*\omega_x$$
$$\Sigma M_z = I_{zz}*\dot{\omega}_z - (I_{xx} - I_{yy})*\omega_x*\omega_y$$

Assuming the reference frame coincides with the principal axes, $I_{xy,xz,yz} = 0$, and assuming $\omega_{x,z} = 0$, yields the following:

$$\int \Sigma M_y \, dt = I_{yy} * \dot{\omega}_y$$
$$\omega_y = 1.12 \text{ rad/sec}$$

APPENDIX C

A. LONGITUDINAL EQUATIONS OF MOTION

The equations of motion for the pod can be derived from Newton's Second Law of motion, which states that the summation of all external forces acting on a body must be equal to the time rate of change of the momentum of the body, and the summation of the external moments acting on a body must be equal to the time rate of change of the moment of momentum (angular momentum). The time rates of change are all taken with respect to body coordinates space. [Ref.8]

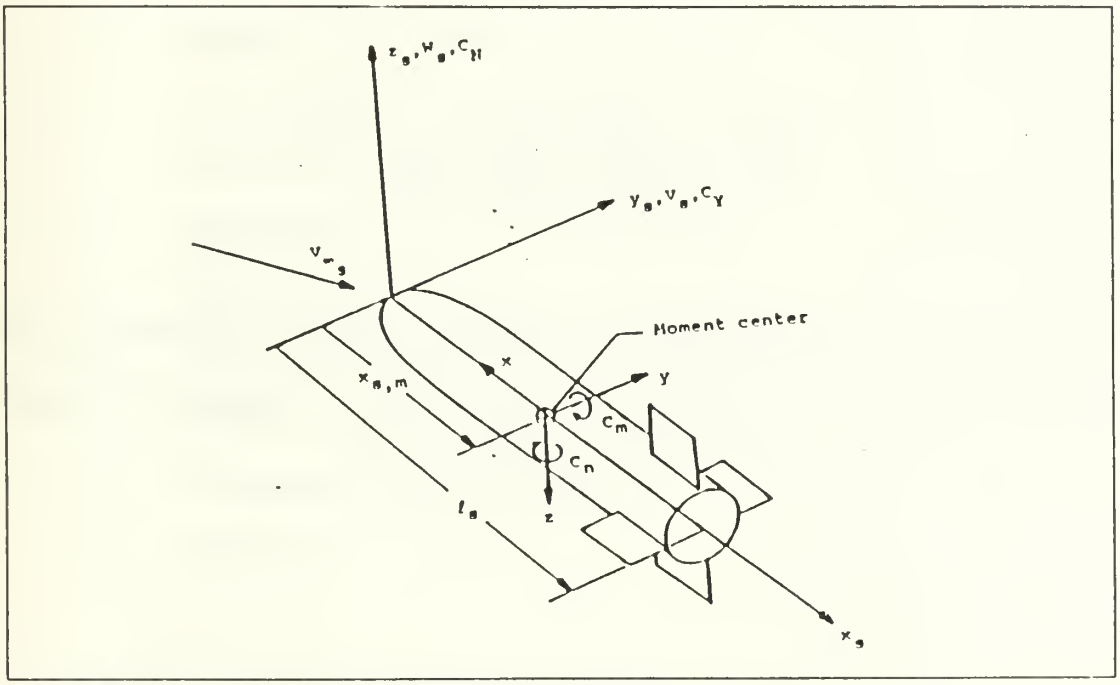

Figure 21 Store Reference Frame

$$\sum \Delta F_x = m*(\dot{U}+W*Q-V*R)$$
$$\sum \Delta F_z = m*(\dot{W}+V*P-U*Q)$$
$$\sum \Delta M = \dot{Q}*I_y+P*R*(I_x-I_z)+(P^2-R^2)*J_{xz}$$

$$\sum \Delta F_x = m*(\dot{U}+W*Q-V*R)$$
$$\sum \Delta F_z = m*(\dot{W}+V*P-U*Q)$$
$$\sum \Delta M = \dot{Q}*I_y$$

By restricting the disturbances to small perturbations about the equilibrium condition, the product of the variations will be small in comparison with the variations and can be neglected, and the small angle assumptions can be made relative to the angles between the equilibrium and disturbed axes.

$$\sum \Delta F_x = m*\dot{u}$$
$$\sum \Delta F_z = m*(\dot{w}-U*q) = m*(\dot{w}-U*\dot{\Theta})$$
$$\sum \Delta M = I_y*\dot{q} = I_y*\ddot{\Theta}$$

Expanding the applied forces and moments in terms of the changes in the aerodynamic and gravitation forces and moments using the total differential form yields:

$$\sum dF_x = (\partial F_x/\partial U) * dU + (\partial F_x/\partial W) * dW + (\partial F_x/\partial \dot{W}) * d\dot{W} + (\partial F_x/\partial \Theta) * d\Theta + (\partial F_x/\partial \Theta$$

$$\sum dF_z = (\partial F_z/\partial U) * dU + (\partial F_z/\partial W) * dW + (\partial F_z/\partial \dot{W}) * d\dot{W} + (\partial F_z/\partial \Theta) * d\Theta + (\partial F_z/\partial \Theta$$

$$\sum \Delta M = (\partial M/\partial U) * dU + (\partial M/\partial W) * dW + (\partial M/\partial \dot{W}) * d\dot{W} + (\partial M/\partial \Theta) * d\Theta$$

Non-dimensionalizing the terms in the above equations yield the aerodynamic coefficients. Following are the definitions of the longitudinal stability coefficients and derivatives:

C_{xu} Variation of drag and thrust with u.

$C_{x\alpha}$ Lift and drag variations along the x-axis.

C_w Gravity

$C_{x\dot{\alpha}}$ Downwash lag on drag.

C_{xq} Effect of pitch rate on drag.

C_{zu} Variation of normal force with u.

$C_{z\alpha}$ Slope of the normal force curve.

$C_{z\dot{\alpha}}$ Downwash lag on lift of tail.

C_{zq} Effect of pitch rate on lift.

C_{mu} Effects of thrust, slipstream, and flexibility.

$C_{m\alpha}$ Static longitudinal stability.

$C_{m\dot{\alpha}}$ Downwash lag on moment.

C_{mq} Damping in pitch.

Arranging the linearized longitudinal equations into matrix form yields the following matrix equation. The control

matrix B is not shown here but is included in the Control-C program. Since there are no active control surfaces, the B-matrix is a zero matrix.

$$\begin{bmatrix} \Delta u \\ \Delta w \\ \Delta q \\ \Delta \theta \end{bmatrix} = \begin{bmatrix} X_u & X_w & 0 & -g \\ Z_u & Z_w & u & 0 \\ M_u+M_w*Z_u & M_w+M_w*Z_w & M_q+M_w*U & 0 \\ 0 & 0 & 0 & 0 \end{bmatrix} \begin{bmatrix} \Delta u \\ \Delta w \\ \Delta q \\ \Delta \theta \end{bmatrix}$$

B. LATERAL EQUATIONS OF MOTION

In the same manner used to obtain the longitudinal equations, the lateral equations are derived. The same assumptions using perturbation theory apply. Following are the equations in their developing order.

$$\sum \Delta F_y = m*(\dot{V}+U*R-W*P)$$
$$\sum \Delta L = \dot{P}*I_x-\dot{R}*J_{xz}+Q*R*(I_z-I_y)-P*Q*J_{xz}$$
$$\sum \Delta N = \dot{R}*I_z+\dot{P}*J_{xz}+P*Q*(I_y-I_x)+Q*R*J_{xz}$$

$$\sum \Delta F_y = m*(\dot{v}+U*r+u*r)$$
$$\sum \Delta L = \dot{p}*I_x-\dot{r}*J_{xz}$$
$$\sum \Delta N = \dot{r}*I_z-\dot{p}*J_{xz}$$

$$\sum \Delta F_y = m*(\dot{v}+U*r)$$
$$\sum \Delta L = \dot{p}*I_x-\dot{r}*J_{xz}$$
$$\sum \Delta N = \dot{r}*I_z-\dot{p}*J_{xz}$$

$$\sum dF_y = (\partial F_y/\partial \mathbf{B})*d\mathbf{B}+(\partial F_y/\partial \Psi)*d\Psi+(\partial F_y/\partial \Phi)*d\Phi+(\partial F_y/\partial \dot{\Phi})*d\dot{\Phi}+(\partial F_y/$$

$$\begin{bmatrix}\Delta\beta\\ \Delta p\\ \Delta r\\ \Delta\phi\end{bmatrix} = \begin{bmatrix}Y_\beta/u & Y_p/u & -(1-Y_r/u) & g*\cos\theta/u\\ L_\beta & L_p & L_r & 0\\ N_\beta & N_p & N_r & 0\\ 0 & 1 & 0 & 0\end{bmatrix} \begin{bmatrix}\Delta\beta\\ \Delta p\\ \Delta r\\ \Delta\phi\end{bmatrix}$$

```
m=input('enter m (lbs):')/32.2;
Uo=input('enter Uo (fps):');
S=input('enter S (in**2):')/144;
b=input('enter b (in):')/12;
Ro=input('enter Ro (slugs/ft**3):');
cref=input('enter c ref(in):')/12;
Ix=input('enter Ixx (ft-lb):')/32.2;
Iy=input('enter IYY (ft-lb):')/32.2;
Iz=input('enter Izz (ft-lb):')/32.2;
g=32.174;
Cn=input('enter Cn (Normal Force coefficient):');
Cm=input('enter Cm (Pitching Moment Coefficient):');
Ca=input('enter Ca (Axial Force Coefficient):');
Cy=input('enter Cy (Side Force Coefficient):');
CLN=input('enter CLN (Yawing Moment Coeff):');
CLL=input('enter CLL (Rolling Moment Coeff):');
CNA=input('enter CNA (Normal Force Deriv wrt AOA):');
CMA=input('enter CMA (Pitching Moment Deriv wrt AOA):');
CYB=input('enter CYB (Side Force Deriv wrt Beta):');
CLNB=input('enter CLNB (yawing Moment deriv wrt Beta);');
CLLB=input('enter CLLB (Rolling Moment deriv wrt Beta):');
CL=input('enter Cl (lift coeff):');
CD=input('enter Cd (Drag coeff):');
CNQ=input('enter CNQ (Normal Force Deriv wrt Q):');
CMQ=input('enter CMQ (Pitching Moment Deriv wrt Q):');
CNAOADOT=input('enter CN AOAdot (Normal Force Deriv wrt AOAdot):');
CMAOADOT=input('enter CM AOAdot (Pitching Mom Deriv wrt AOAdot):');
q=.5*ro*uo*uo;
Xu=-2*Cd*q*s/(m*uo);
Xw=Cl*q*s/(m*uo);
Zu=-2*Cl*q*s/(m*uo);
Zw=-Cd*q*s/(m*uo);
Zwd=Cnaoadot*cref*s*q/(2*uo*uo*m);
Mw=Cma*q*s*cref/(Iy*uo);
Mu=0;
Ma=uo*Mw;
Mwd=Cmaoadot*cref*q*s*cref/(2*uo*uo*Iy);
Mad=uo*Mwd;
Mq=Cmq*cref*q*s*cref/(2*uo*Iy);
A=[Xu Xw 0 -g;Zu Zw uo 0;(Mu+Mwd*Zu)/(1-Zwd) (Mw+Mwd*Zw)/(1-Zwd)...
  (Mq+Mwd*uo)/(1-Zwd) 0;0 0 1 0];
B=[0 0 0 0;0 0 0 0]';C=[0 1 0 0];D=[0 0];
IC=[0 0 0 0]';
IC(2)=input('enter initial vertical velocity (fps):');
IC(3)=input('enter initial pitching rate (rad/s):');
ttt=input('enter end time (sec)');
t=0:.001:ttt;
uuu=(ttt/.001)+1;
u=0*ones(2,uuu);
simu('IC',IC);
y=simu(a,b,c,d,u,t);
erase;
plot(t,y);
```

Figure 22 Control-C Program For EOM Simulation

APPENDIX E

```
                    THE USAF AUTOMATED MISSILE DATCOM A REV  7/89 A
                    AERODYNAMIC METHODS FOR MISSILE CONFIGURATIONS
                                CASE INPUTS

FOLLOWING ARE THE CARDS INPUT FOR THIS CASE

CASEID SIMPLE BODY CONFIGURATION FULL LAT
DERIV RAD
DIM IN
DAMP
 $ELTCON MACH=1.,MACH=0.7,
         REN=4.13E6,
         ALPHA=4.,ALPHA=0.,0.5,1.,2.,3.,4.,BETA=-0.5,$
 $REFQ XCG=63.75,$
 $AXIBOD LNOSE=24.,DNOSE=19.3,LCENTR=83.2,DCENTR=19.3,TAIL=0.,
     LAFT=46.6,DAFT=1.0,$
BUILD
PRINT AERO BODY
PRINT GEOM BODY
NEXT CASE

A WARNING A THE REFERENCE AREA IS UNSPECIFIED, DEFAULT VALUE ASSUMED

A WARNING A THE REFERENCE LENGTH IS UNSPECIFIED, DEFAULT VALUE ASSUMED

THE BOUNDARY LAYER IS ASSUMED TO BE TURBULENT OVER ALL COMPONENTS OF THE CONFIGURATION

THE INPUT UNITS ARE IN INCHES, THE SCALE FACTOR IS   1.0000
```

Figure 23 MISDATCOM INPUT/OUTPUT

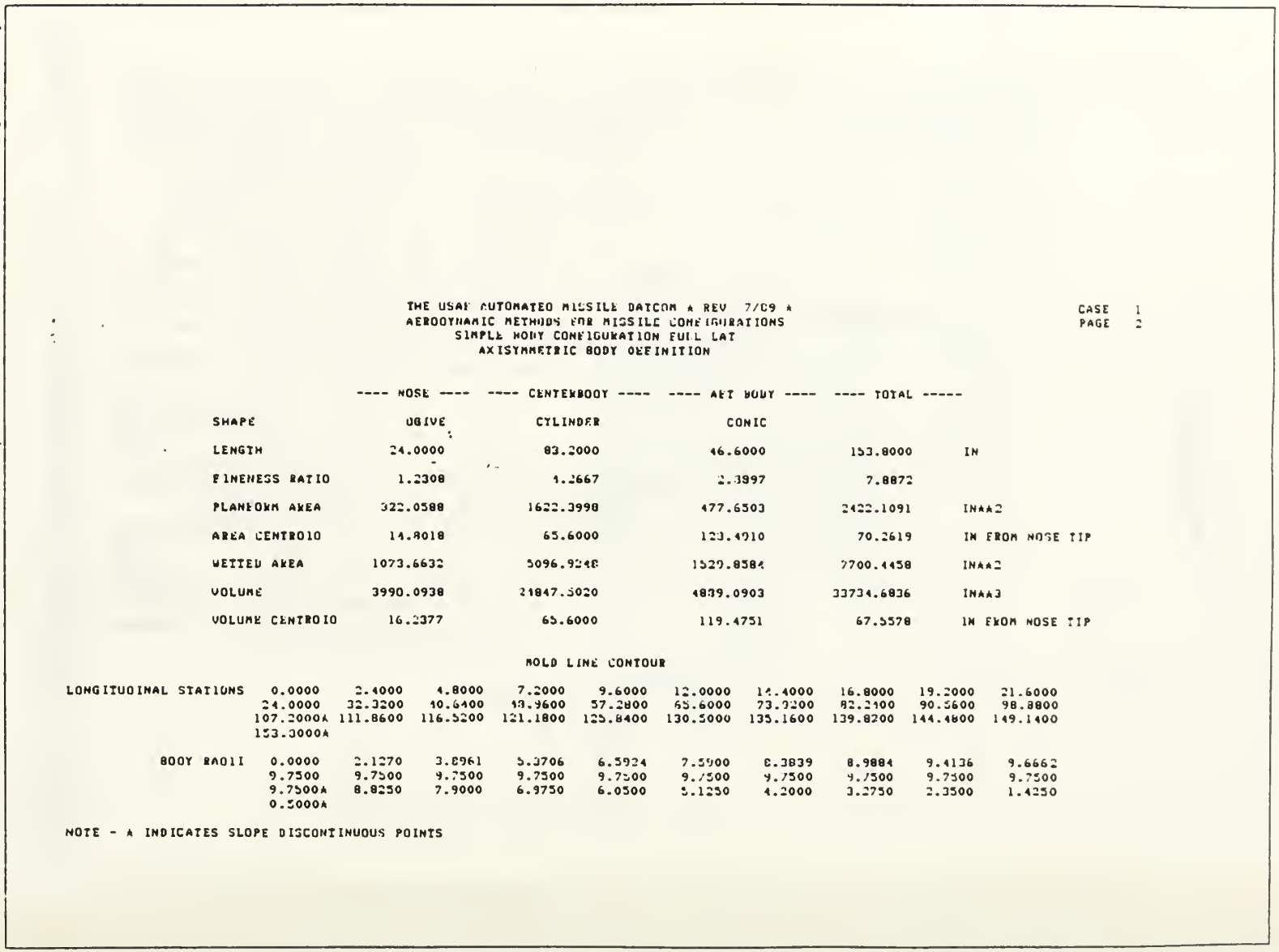

THE USAF AUTOMATED MISSILE DATCOM A REV 7/89 A
AERODYNAMIC METHODS FOR MISSILE CONFIGURATIONS
SIMPLE BODY CONFIGURATION FULL LAT
AXISYMMETRIC BODY DEFINITION

CASE 1
PAGE 2

	---- NOSE ----	---- CENTERBODY ----	---- AFT BODY ----	---- TOTAL -----	
SHAPE	OGIVE	CYLINDER	CONIC		
LENGTH	24.0000	83.2000	46.6000	153.8000	IN
FINENESS RATIO	1.2308	4.2667	2.3897	7.8872	
PLANFORM AREA	322.0588	1622.3998	477.6503	2422.1091	INAA2
AREA CENTROID	14.8018	65.6000	123.4910	70.2619	IN FROM NOSE TIP
WETTED AREA	1073.6632	5096.9248	1529.8584	7700.4458	INAA2
VOLUME	3990.0938	21847.5020	4839.0903	33734.6836	INAA3
VOLUME CENTROID	16.2377	65.6000	119.4751	67.5578	IN FROM NOSE TIP

BOLD LINE CONTOUR

LONGITUDINAL STATIONS	0.0000	2.4000	4.8000	7.2000	9.6000	12.0000	14.4000	16.8000	19.2000	21.6000
	24.0000	32.3200	40.6400	48.9600	57.2800	65.6000	73.9200	82.2400	90.5600	98.8800
	107.2000A	111.8600	116.5200	121.1800	125.8400	130.5000	135.1600	139.8200	144.4800	149.1400
	153.8000A									
BODY RADII	0.0000	2.1270	3.8961	5.3706	6.5924	7.5900	8.3839	8.9884	9.4136	9.6662
	9.7500	9.7500	9.7500	9.7500	9.7500	9.7500	9.7500	9.7500	9.7500	9.7500
	9.7500A	8.8250	7.9000	6.9750	6.0500	5.1250	4.2000	3.2750	2.3500	1.4250
	0.5000A									

NOTE - A INDICATES SLOPE DISCONTINUOUS POINTS

Figure 24 MISDATCOM Input/Output (Cont)

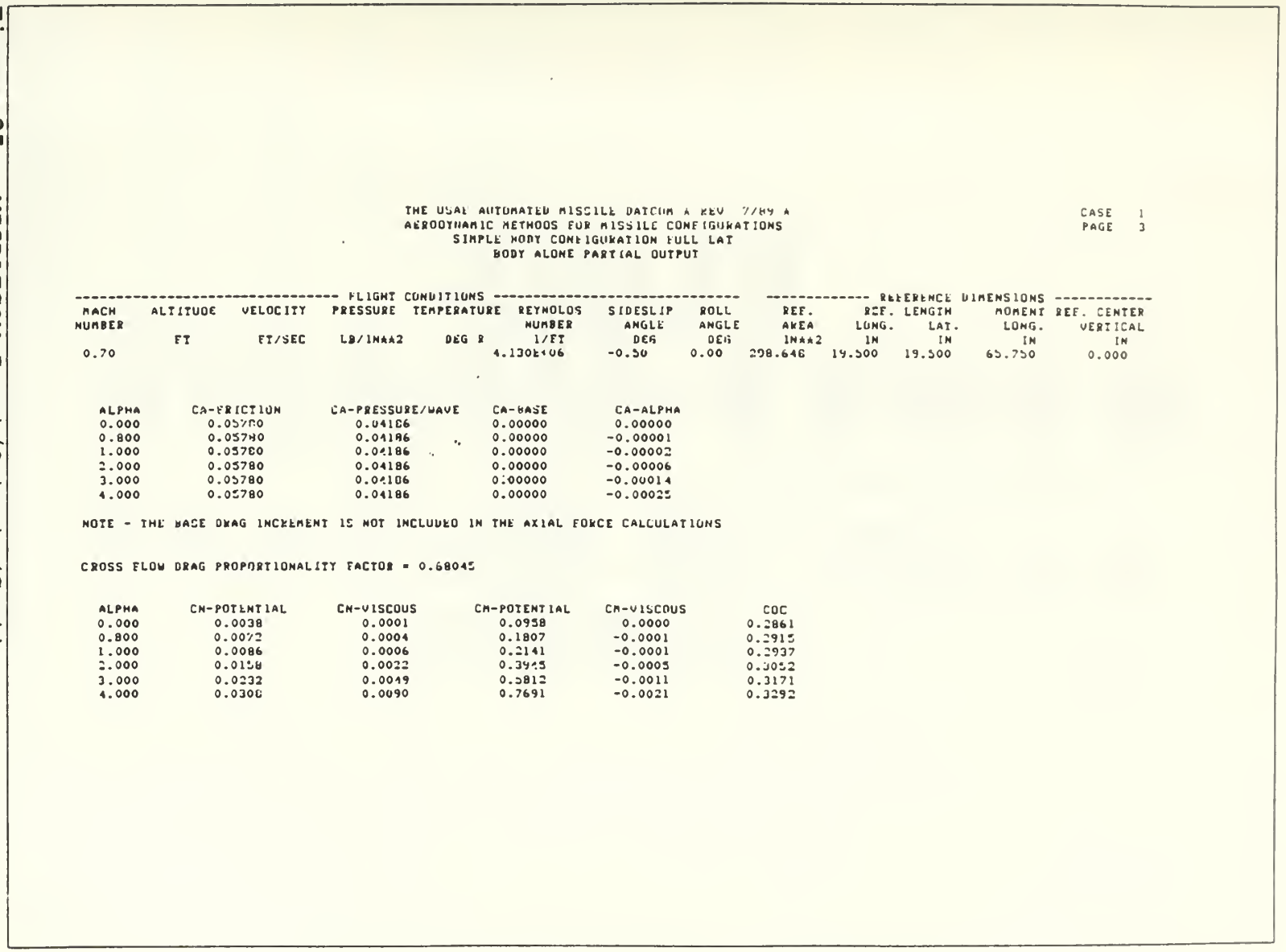

THE USAF AUTOMATED MISSILE DATCOM A REV 7/89 A
AERODYNAMIC METHODS FOR MISSILE CONFIGURATIONS
SIMPLE BODY CONFIGURATION FULL LAT
BODY ALONE PARTIAL OUTPUT

CASE 1
PAGE 3

FLIGHT CONDITIONS								REFERENCE DIMENSIONS				
MACH NUMBER	ALTITUDE FT	VELOCITY FT/SEC	PRESSURE LB/INAA2	TEMPERATURE DEG R	REYNOLDS NUMBER 1/FT	SIDESLIP ANGLE DEG	ROLL ANGLE DEG	REF. AREA INAA2	REF. LENGTH LONG. IN	REF. LENGTH LAT. IN	MOMENT REF. CENTER LONG. IN	MOMENT REF. CENTER VERTICAL IN
0.70					4.130E+06	-0.50	0.00	298.646	19.500	19.500	65.750	0.000

ALPHA	CA-FRICTION	CA-PRESSURE/WAVE	CA-BASE	CA-ALPHA
0.000	0.05780	0.04186	0.00000	0.00000
0.800	0.05780	0.04186	0.00000	-0.00001
1.000	0.05780	0.04186	0.00000	-0.00002
2.000	0.05780	0.04186	0.00000	-0.00006
3.000	0.05780	0.04186	0.00000	-0.00014
4.000	0.05780	0.04186	0.00000	-0.00025

NOTE - THE BASE DRAG INCREMENT IS NOT INCLUDED IN THE AXIAL FORCE CALCULATIONS

CROSS FLOW DRAG PROPORTIONALITY FACTOR = 0.68045

ALPHA	CN-POTENTIAL	CN-VISCOUS	CM-POTENTIAL	CM-VISCOUS	COC
0.000	0.0038	0.0001	0.0958	0.0000	0.2861
0.800	0.0072	0.0004	0.1807	-0.0001	0.2915
1.000	0.0086	0.0006	0.2141	-0.0001	0.2937
2.000	0.0158	0.0022	0.3945	-0.0005	0.3052
3.000	0.0232	0.0049	0.5812	-0.0011	0.3171
4.000	0.0308	0.0090	0.7691	-0.0021	0.3292

Figure 25 MISDATCOM Input/Output (Cont)

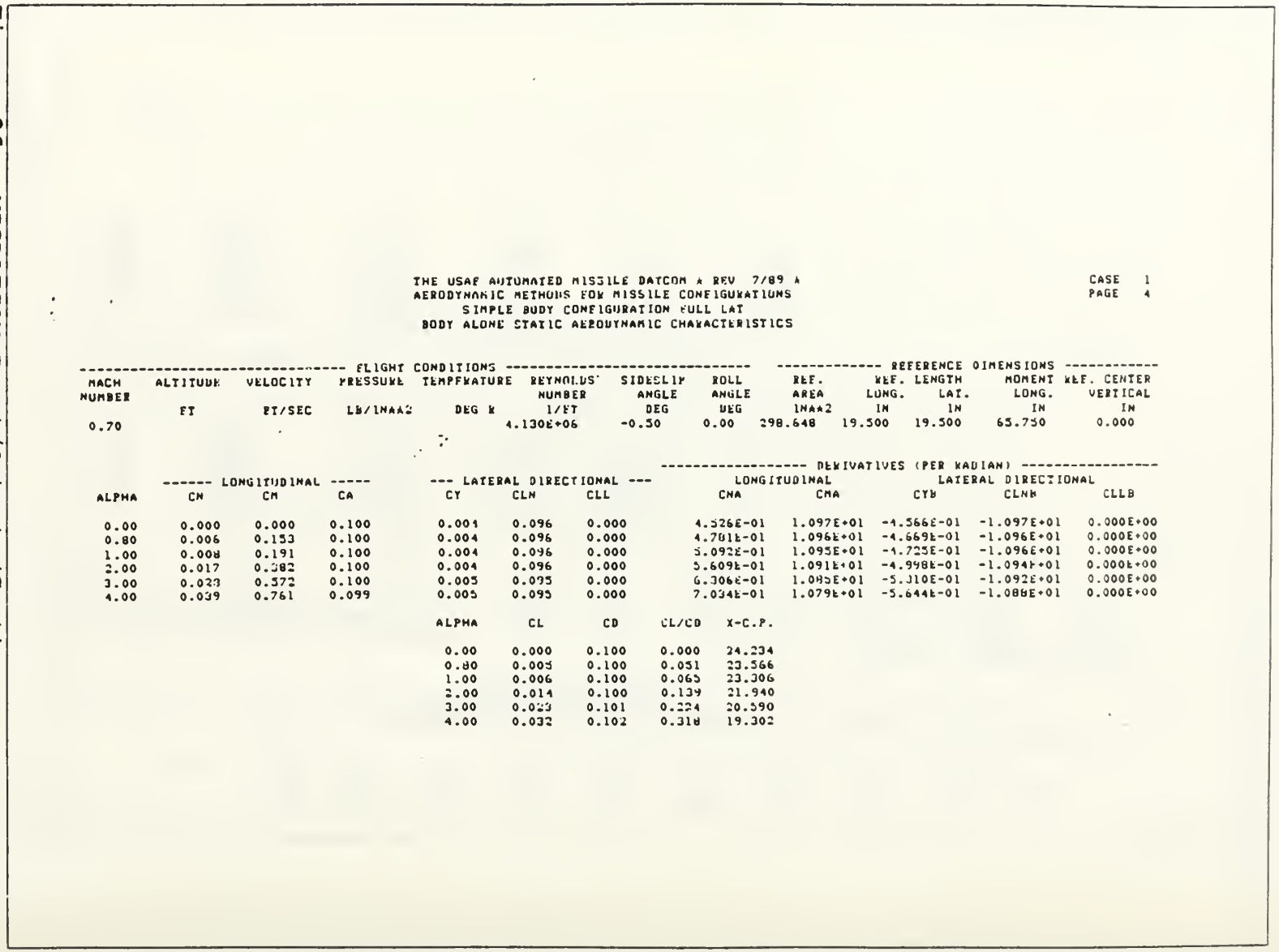

THE USAF AUTOMATED MISSILE DATCOM * REV 7/89 *
AERODYNAMIC METHODS FOR MISSILE CONFIGURATIONS
SIMPLE BODY CONFIGURATION FULL LAT
BODY ALONE STATIC AERODYNAMIC CHARACTERISTICS

CASE 1
PAGE 4

FLIGHT CONDITIONS

MACH NUMBER	ALTITUDE FT	VELOCITY FT/SEC	PRESSURE LB/INAA2	TEMPERATURE DEG R	REYNOLDS NUMBER 1/FT	SIDESLIP ANGLE DEG	ROLL ANGLE DEG
0.70					4.130E+06	-0.50	0.00

REFERENCE DIMENSIONS

REF. AREA INAA2	REF. LENGTH LONG. IN	REF. LENGTH LAT. IN	MOMENT REF. LONG. IN	REF. CENTER VERTICAL IN
298.648	19.500	19.500	65.750	0.000

DERIVATIVES (PER RADIAN)

ALPHA	LONGITUDINAL CN	LONGITUDINAL CM	LONGITUDINAL CA	LATERAL DIRECTIONAL CY	LATERAL DIRECTIONAL CLN	LATERAL DIRECTIONAL CLL
0.00	0.000	0.000	0.100	0.004	0.096	0.000
0.80	0.006	0.153	0.100	0.004	0.096	0.000
1.00	0.008	0.191	0.100	0.004	0.096	0.000
2.00	0.017	0.382	0.100	0.004	0.096	0.000
3.00	0.023	0.572	0.100	0.005	0.095	0.000
4.00	0.039	0.761	0.099	0.005	0.095	0.000

ALPHA	LONGITUDINAL CNA	LONGITUDINAL CMA	LATERAL DIRECTIONAL CYB	LATERAL DIRECTIONAL CLNB	LATERAL DIRECTIONAL CLLB
	4.526E-01	1.097E+01	-4.566E-01	-1.097E+01	0.000E+00
	4.701E-01	1.096E+01	-4.669E-01	-1.096E+01	0.000E+00
	5.092E-01	1.095E+01	-4.725E-01	-1.096E+01	0.000E+00
	5.609E-01	1.091E+01	-4.998E-01	-1.094E+01	0.000E+00
	6.306E-01	1.085E+01	-5.310E-01	-1.092E+01	0.000E+00
	7.034E-01	1.079E+01	-5.644E-01	-1.088E+01	0.000E+00

ALPHA	CL	CD	CL/CD	X-C.P.
0.00	0.000	0.100	0.000	24.234
0.80	0.005	0.100	0.051	23.566
1.00	0.006	0.100	0.065	23.306
2.00	0.014	0.100	0.139	21.940
3.00	0.023	0.101	0.224	20.590
4.00	0.032	0.102	0.318	19.302

Figure 26 MISDATCOM Input/Output (Cont)

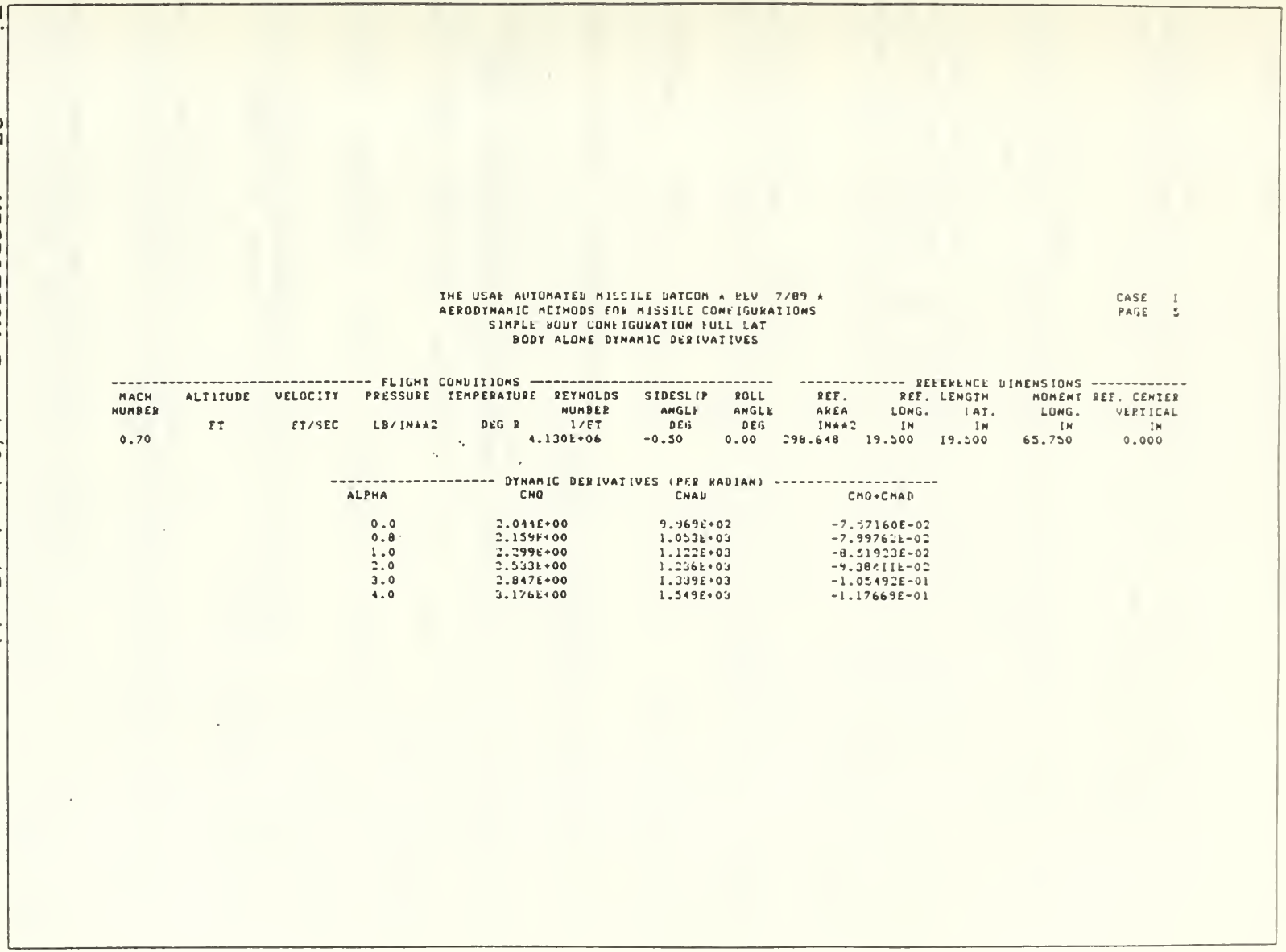

THE USAF AUTOMATED MISSILE DATCOM * REV 7/89 *
AERODYNAMIC METHODS FOR MISSILE CONFIGURATIONS
SIMPLE BODY CONFIGURATION FULL LAT
BODY ALONE DYNAMIC DERIVATIVES

CASE 1
PAGE 5

FLIGHT CONDITIONS								REFERENCE DIMENSIONS			
MACH NUMBER	ALTITUDE FT	VELOCITY FT/SEC	PRESSURE LB/INAA2	TEMPERATURE DEG R	REYNOLDS NUMBER 1/FT	SIDESLIP ANGLE DEG	ROLL ANGLE DEG	REF. AREA INAA2	REF. LENGTH LONG. IN	LAT. IN	MOMENT LONG. IN	REF. CENTER VERTICAL IN
0.70					4.130E+06	-0.50	0.00	298.648	19.500	19.500	65.750	0.000

DYNAMIC DERIVATIVES (PER RADIAN)

ALPHA	CNQ	CNAD	CNQ+CNAD
0.0	2.044E+00	9.969E+02	-7.37160E-02
0.8	2.159E+00	1.053E+03	-7.99762E-02
1.0	2.299E+00	1.122E+03	-8.51923E-02
2.0	2.533E+00	1.236E+03	-9.38411E-02
3.0	2.847E+00	1.389E+03	-1.05492E-01
4.0	3.176E+00	1.549E+03	-1.17669E-01

Figure 27 MISDATCOM Input/Output (Cont)

LIST OF REFERENCES

1. Mendenhall, M.R., Lesieutre, D.J., Caruso, S.C., Dillinius, M.F.E., Kuhn, G.D., *Aerodynamic Design of Pegasus*, CP-493, paper presented at the AGARD Conference Proceedings #493, pages 7-1,2.

2. Air Force Flight Dynamics Laboratory, AFWAL-TR-86-3091, *Missile Datcom, Volume I- Final Report*, Vukelich, S.R., Stoy, S.L., Bruns, K.A., Castillo, J.A., Moore, M.E., December 1988.

3. Air Force Flight Dynamics Laboratory, Technical Report AFFDL-TR-72-83, Vol. I, 1972, *Prediction of the Six-Degree-of-Freedom Store Separation Trajectories at Speeds up to the Critical Speed, Vol. I--Theoretical methods and Comparisons with Experiment*, by Dillenius, M.F.E., Goodwin, F.K., and Nielsen, J.N., 1972.

4. Joint Ordnance Commander Subgroup For Aircraft/Stores Compatibility, AOP-12, Volume 3, *Aircraft Stores Interface Manual*, pp. 2-(15-18), April, 1983.

5. CricketGraph® software, copyright 1990, Computer Associates.

6. Nelson, R.C., *Flight Stability and Automatic Control*, page 113, McGraw-Hill Book Co., 1989.

7. Dickenson, B., *Aircraft Stability and Control for Pilots and Engineers*, p. 14, Pitman Publishing Corporation, 1968.

8. PC-MATLAB Version 3.2-PC software, copyright 1987, The MathWorks, Inc.

9. Ctrl-C software, copyright 1986, Systems Control Technology, Inc.

10. Spahr, H. R., *Theoretical Store Separation Analysis of a Prototype Store*, Journal of Aircraft, Volume 12, Number 10, page 807, October 1975.

11. van den Broek, G. J., *The Use of a Panel Method in the Prediction of External Store Separation*, Journal of Aircraft, Volume 21, Number 5, page 309, May 1984.

12. Miranda, L. R., *Extended Applications of the Vortex Lattice Method*, Vortex Lattice Utilization, NASA SP-405, page 27, 1984.

13. Bertin, J. J., Smith, M. L., *Aerodynamics for Engineers*, Prentice-Hall, Incorporated, 1989.

INITIAL DISTRIBUTION LIST

		No. Copies
1.	Defense Technical Information Center Cameron Station Alexandria, VA 22304-6145	2
2.	Library, Code 52 Naval Postgraduate School Monterey, CA 93943-5002	2
3.	Chairman Department of Aeronautics and Astronautics Naval Postgraduate School Monterey, CA 93943-5000	1
4.	Commander Pacific Missile Test Center Point Mugu, CA 93042	1
5.	Naval Air Systems Command AIR-530E Washington, D.C. 20361	1
6.	Flight Dynamics Laboratory Air Force Wright Aeronautical Laboratories Air Force Systems Command ATTN: Mr. William Blake Wright Patterson Air Force Base, OH 45433-6553	1
7.	Naval Weapons Center Code 3592 ATTN: Mr. L. Gleason China Lake, CA 93555	1
8.	Pacific Missile Test Center Code 9053 Point Mugu, CA 93042	4
9.	Prof. O. Biblarz, Code AA/Bi Department of Aeronautics and Astronautics Naval Postgraduate School Monterey, CA 93942-5000	1
10.	Prof. L. Schmidt, Code AA/Si Department of Aeronautics and Astronautics Naval Postgraduate School Monterey, CA 93942-5000	1

Thesis
H201235 Hansen
c.1 Store separation
methodology analysis.